Mathematical Biosciences 350 (2022) 108832

Contents lists available at ScienceDirect

Mathematical Biosciences

journal homepage: www.elsevier.com/locate/mbs

Original Research Article

Investigating the impact of multiple feeding attempts on mosquito dynamics via mathematical models

Bime M. Ghakanyuy [a], Miranda I. Teboh-Ewungkem [b], Kristan A. Schneider [c], Gideon A. Ngwa [a,*]

[a] Department of Mathematics, University of Buea, P.O. Box 63, Buea, Cameroon
[b] Department of Mathematics, Lehigh University, Bethlehem, PA, 18015, USA
[c] Department of Applied Computer and Bio-Sciences, University of Applied Sciences, Mittweida, Technikumplatz 17, 09648 Mittweida, Germany

ARTICLE INFO

Keywords:
Mosquito dynamics
Multiple feeding attempts
Transitions
Gonotrophic cycle
Stable and unstable manifold
Hopf bifurcation

ABSTRACT

A deterministic differential equation model for the dynamics of terrestrial forms of mosquito populations is studied. The model assesses the impact of multiple probing attempts by mosquitoes that quest for blood within human populations by including a waiting class for mosquitoes that failed a blood feeding attempt. The equations are derived based on the idea that the reproductive cycle of the mosquito can be viewed as a set of alternating egg laying and blood feeding outcomes realised on a directed path called the gonotrophic cycle pathway. There exists a threshold parameter, the basic offspring number for mosquitoes, whose nature is affected by the way we interpret the transitions involving the different classes on the gonotrophic cycle path. The trivial steady state for the system, which always exists, can be globally asymptomatically stable whenever the threshold parameter is less than unity. The non-trivial steady state, when it exists, is stable for a range of values of the threshold parameter but can also be driven to instability via a Hopf bifurcation. The model's output reveals that the waiting class mosquitoes do contribute positively to sustain mosquito populations as well as increase their interactions with humans via increased frequency and initial amplitude of oscillations. We conclude that to understand human–mosquito interactions, it is informative to consider multiple probing attempts; known to occur when mosquitoes quest for blood meals within human populations.

1. Introduction

Mosquitoes are the agents responsible for the transmission of several vector-borne diseases, for example malaria, the deadliest of them all, dengue fever, yellow fever, Zika, West Nile, lymphatic filariasis (elephantiases), and more [1–5]. A successful transmission of the pathogens, be it a parasite or a virus, that cause the aforementioned human diseases, requires a successful interaction between a mosquito and the host. By success, we mean an interaction between humans and mosquitoes that leads to disease transfer. Thus, in the context of mosquito borne infections of humans, human–mosquito interaction is an important link to disease transmission success. See, for example, [6–10], for some ideas on this.

To fight mosquito-borne diseases, continuous efforts and monitoring is needed from both the public health officials in the countries most affected by the diseases and WHO. Firstly, regions previously uninhabitable by disease transmitting mosquitoes are becoming more suitable as habitats for these disease mosquitoes, exacerbated by global warming threats as reported for dengue and chikungunya virus vectors (Aedes species mosquitoes) [11–13] and Japanese Encephalitis (JE) virus vectors in Asia (culex species mosquito) [14]. In particular, global warming and shifting climatic patterns have been reported to affect both the abundance and redistribution of these vector-borne disease mosquitoes, and these have severe consequences for disease transmission [12,15,16]. Secondly, due to the COVID-19 pandemic, there are concerns that pre-pandemic control programs for mosquito-borne diseases may be affected [17,18] with the potential for a reduction in funding due to the COVID-19 related economic impacts and difficulties. Some of these vector-borne disease-related control programs seek to reduce vector abundance and/or competence via mechanistic or chemical means [3,19,20] or disrupt and minimise contacts between vectors and the vertebrates affected/infected by pathogens transmitted by the vectors [21]. Methods employed include the use of screens to protect vector entry into habitats, and/or the use of insecticide treated bednets aimed to kill vectors that enter residences; removal of vector breeding habitats from around vertebrate habitats; the use of larvicides applied at breeding sites aimed at reducing or destroying the aquatic life-forms, progenies of adult mosquitoes [22]; infusion of predators that feed on the progeny of the adult mosquitoes at mosquito breeding sites [23], and increasingly, the use of genetically modified (GM) mosquitoes to reduce the size of breeding adult mosquitoes and hence total mosquito

* Corresponding author.
E-mail address: gideon.ngwa@ubuea.cm (G.A. Ngwa).

https://doi.org/10.1016/j.mbs.2022.108832
Received 8 July 2021; Received in revised form 7 April 2022; Accepted 9 May 2022
Available online 17 June 2022

population [5,19,24]. Additionally, Intermittent Preventive Treatment (IPT) is a preventative tool utilised in some endemic countries in which at risk non symptomatic individuals (infectious or not) are given a therapeutic dose of an antimalarial medication [25,26]. In situations where transmission of the pathogen has succeeded, particularly for human diseases like malaria and Zika, complete and timely treatment of the infectious individual is necessary so as to terminate the pathogen's cycle [21,26].

It is thus clear that any control of vector-borne diseases requires an Integrated Vector Management (IVM) approach, embedded with a human disease management strategy, together with an understanding of environmental drivers and factors that can hinder a successful implementation of the said control strategies. The successes of such a holistic and comprehensive control method requires a deeper understanding of the facets of the interaction among vectors, humans and pathogens; how their interaction enhances the successes of the pathogen and the transmitting vector and how such an interaction can be exploited for a more efficient and successful control. With vectors the drivers of such diseases via their interaction with humans for blood like in the case of malaria, and hence an ubiquitous component in the disease control problem, it is essential to understand their population dynamics and characterise the factors that could affect their size, abundance and survival. Furthermore, given that empirical studies aimed at monitoring human–mosquito interaction are relatively difficult, mathematical models developed to capture these interactive dynamics between mosquitoes and humans with the mosquitoes seen as the drivers are not only necessary but important and urgent. With this is mind, we set out to accomplish this task focusing on mosquito vectors, and for the most part, using the malaria mosquito as our model example; but the ideas can be transferred to other mosquito vectors with appropriate modifications.

Mosquitoes that transmit pathogens from one human to another are the breeding mosquitoes, which are the female mosquitoes, when they bite humans to harvest blood for the maturation of their eggs, forming the disease infection pathway from humans to mosquitoes and from mosquitoes back to humans. The entire cycle from a bloodmeal to oviposition is known as the *gonotrophic cycle*, and is typically repeated by an adult female mosquito throughout its lifetime [5]. Thus, transmission in humans is essentially driven by these female mosquitoes through their *human-biting habit*, in search for a bloodmeal. For malaria, these are the female *Anopheles sp* mosquitoes; for Zika virus disease, the *Aedes sp* mosquitoes are the primary route of disease infection in humans, precisely (*Aedes aegypti* and *Aedes albopictus*), same mosquitoes responsible for the spread of yellow fever, dengue and chikungunya viruses [13,27]. With focus on the malaria mosquito, the human-biting habit of the female *Anopheles sp* mosquito, which has been interpreted as a restricted form of homogeneous mixing and used successfully in deriving models for transmission of malaria, [6,7,28–32], requires that she visits and bites humans from time to time to harvest the blood which she needs for the maturation of her eggs. During the blood feeding encounter, the human can infect the questing mosquito or vice-visa depending on the health status of the human and mosquito. It is with this understanding that some authors, including [9,10,33–36], have considered only the population density of female mosquitoes in modelling mosquito dynamics. Those authors partitioned the female mosquito population into classes representing physiological status when considering the demographics model for the population dynamics of mosquitoes. One such partition often used is that of (i) aquatic forms of the mosquito, (ii) newly emerged and hungry adult forms of the mosquitoes, (iii) fertilised adult mosquitoes questing for blood in human habitat areas, and (iv) well blood-fed and resting adult mosquitoes [3,20,35,37].

In several of the studied compartmental demographic models for mosquito population dynamics, it is assumed that during questing, a questing mosquito can either succeed to feed and survive with probability p or gets killed with probability $1-p$. This binary success-failure assumption that results in the death of the questing mosquito in the case of failure of a feeding attempt is not realistic. There can be multiple reasons, including interruptions of several types, which may lead to failure to feed by the questing mosquito but not resulting in its death. We expect, instead, that an evolutionary reproductive need would drive the questing mosquito that survives an unsuccessful feeding encounter, to attempt to blood-feed again as often as is required, if each previous questing attempt to get a satisfactory amount of blood from the human was unsuccessful. In fact, there is evidence, that questing mosquitoes do harvest more than one blood meal before entering the resting phase of their gonotrophic cycle [38]. Multiple blood meals during a single gonotrophic cycle can have consequences in the spread of malaria in the sense that an infected and infectious questing mosquito that takes blood from two different susceptible humans can successfully infect both humans during one gonotrophic cycle, raising the possibility of multiple infection transfers in one mosquito outing. In [3], it is argued that for the malaria parasite to be transmitted from one human to the next, the infecting mosquito must bite two different humans at two distinct times, emphasising, in another sense, the necessity of multiple bites from the questing mosquitoes. In this paper, we shall extend the model presented in [9] to include the possibility of multiple feeding attempts by each questing mosquito. The main objective of the current manuscript is therefore to further interpret the life style of the mosquito to include the fact that the mosquito can perform multiple feeding attempts during one questing episode until it harvests the required amount of blood that it needs to be able to complete a gonotrophic cycle. An expected outcome of the improved model is an improved version of the basic offspring number for the mosquito population dynamics as well as to provide a platform towards a better understanding of the transmission potential of pathogens by mosquitoes.

The rest of the paper is organised as follows. In Section 2, we derive the model for repeated feeding attempts by mosquitoes based on the earlier models. Here, we also examine the basic properties of the derived model and perform a re-parameterisation to align the system's equations with earlier models. In Section 3 we present a mathematical analysis of the model's equations. In particular we discuss the existence and stability of steady state solutions and in the process identify the possible threshold parameters that exist in the model. In this section, we link the identified threshold parameter with the *basic offspring number for mosquitoes*. In Section 4, we examine in detail how the multiple feeding paradigm affects the mosquito dynamic, in more complex ways than when not considered. We round up the paper with a discussion and conclusion in Section 5.

2. The mathematical model development

We start by noting that during the periods of time when female breeding mosquitoes are most active, they systematically seek vertebrates, including humans, to harvest blood, [39]. We refer to the class of mosquitoes out in search for a blood meal as questing mosquitoes. If a questing mosquito is interrupted while attempting to take a blood meal, we assume that if the mosquito survives the attempted feeding encounter, it will simply try again to blood feed either on the same or a different blood source, depending on the prevailing circumstances. We assume in general that a questing mosquito will repeatedly quest for blood until it succeeds in harvesting the required and satisfactory blood meal or dies in the process.

We divide the female mosquito population into four classes representing physiological status so that at each time t we have the following classes of mosquitoes: (i) *Breeding site mosquitoes*: These are the newly emerged adult female mosquitoes together with any older mosquitoes that have returned to the breeding site to lay eggs, denoted by B; (ii) *Questing mosquitoes*: These are the fertilised adult mosquitoes that have left the breeding site and are now questing for blood within human populations, denoted by Q; (iii) *Resting mosquitoes:* These are the blood-fed mosquitoes that have successfully harvested blood (from humans)

and because they are well fed are now resting in view of returning to the breeding site to lay eggs, denoted by R and (iv) *Waiting class mosquitoes:* They are mosquitoes that have tried but survived a failed attempt to take a blood meal and are now in a waiting class, denoted by W. The mosquitoes in the W class will then be re-attracted to humans again for a second and subsequent questing attempt. The new addition here is the waiting class mosquitoes and it comprises all type Q mosquitoes that were interrupted during a feeding episode and who survived the failed feeding attempt. Thus the total mosquito population at time, t is $T_m(t) = B(t)+Q(t)+R(t)+W(t)$. As in [8,9], we assume that the newly emerged adults get fertilised before they can proceed to quest for a blood meal. It is well known to biologist that blood contains the necessary proteins needed for the maturation of eggs within the female mosquito, and that autogenous and anautogenous mosquitoes respond to this blood feeding need differently [5,40,41]. Thus, while some obligate autogenous mosquitoes can develop eggs without a vertebrate blood meal, all anautogenous and facultative autogenous mosquitoes require blood, at one stage or the other, for the maturation of a clutch of eggs. Questing for blood within vertebrate populations is thus vital for mosquito survival. We thus assume that new births are only possible after a successful questing episode. Once type B vectors arrive at the human habitat site, they become type Q i.e. questing mosquitoes. They quest with probability of success p and failure $1-p$. We shall equally assume that interaction between mosquitoes and humans is via mass action contact. If the questing is successful, we have resting mosquitoes, R, else the surviving mosquitoes after the unsuccessful questing episode are moved into the waiting class W. We assume at all time the presence of humans in the system with constant density H, as well as the possibility for mosquitoes seeking alternative sources[1] for a blood meal via the presence of the parameter K. The different state variables used in this model are defined in Table 1 and parameter description in Table 2.

Mosquitoes of type R return to the breeding site at the rate a to lay eggs. We assume that the link between adult mosquitoes of the current generation and new adults is via the reproductive output of the vectors of type R, and that each type R mosquito produces new offspring at rate $\lambda(R)$ where $\lambda : [0,\infty) \to \mathbb{R}$ is a suitably defined function which we refer to as the birth rate function. The assumption is that each vector of type R produces $\lambda(R)$ new offspring so that all R mosquitoes produce $R\lambda(R)$ new vectors and flow to the breeding site at rate a. We use the same restrictions as in Teboh-Ewungkem et *al.*, [3], to have the following definition for a suitable birth rate function.

Definition 2.1 (*Suitable Birth Rate Function*). A function $\lambda : [0,\infty) \longrightarrow \mathbb{R}$ is a suitable birth rate function if it satisfies the following assumptions:

A1: λ is continuous on $[0,\infty)$ with $\lambda(0+) = \lim_{R\to 0+}\lambda(R) = \lambda(0) = \lambda_0 > 0$.

A2: λ is differentiable in $(0,\infty)$ with $\lambda'(R) < 0$ for all $R \geq 0$.

A3: $\lambda_\infty = \lim_{R\to\infty}\lambda(R) < \lim_{R\to 0+}\lambda(R) = \lambda(0+) = \lambda_0$.

A4: The function $R\lambda(R)$, which is continuous and differentiable, is bounded above and unimodal with a global maximum and turning point at $R = R_m$ so that $R_m\lambda(R_m) = \lambda_m$ where $0 < \lambda_m < \infty$.

Assumptions $A1$ and $A3$ will allow us to select only the birth rate function λ that is continuous on $[0,\infty)$ and differentiable in $(0,\infty)$ while A2 guarantees that $\lambda^{-1}(R)$ exists for any $R > 0$. Assumption $A4$ is designed to ensure that if we consider a recruitment-death process with per capita death rate μ_R, modelled by the equation $R'(t) = R\lambda(R)-\mu_R R$, then in addition to the trivial steady state solution $R^* = 0$, a unique non-zero steady state solution exists, defined by the equation $\lambda(R^*) - \mu_R = 0$. Its value for any $\mu_R \in (0,\lambda_0)$ will be given by $R^* = \lambda^{-1}(\mu_R)$, which is globally and asymptotically stable. Examples of $\lambda(R)$ are

$$(a)\ \ \lambda(R) = \lambda_0\left(1-\frac{R}{L_v}\right); \qquad (b)\ \ \lambda(R) = \frac{\lambda_0}{1+\left(\frac{R}{L_m}\right)^n},\ n \geq 1; \qquad (c)\ \ \lambda(R) = \lambda_0 e^{-\frac{R}{L_r}}, \tag{1}$$

where L_v, L_m and L_r are positive constants that can be arbitrarily large. In each of these examples, we expect $R \in [0, L)$ where $L \in \{L_v, L_m, L_r\}$, $L \gg 0$ can be identified with the carrying capacity of the environment in question while $\lambda_0 > 0$ may be regarded as the limiting rate at which type R mosquitoes would lay eggs, if the population of these types of mosquitoes should become very small. Formulas (a) and (c) satisfy $A1-A4$ above. For formulas (b) and (c), $\lambda(R) > 0$ and $\lim_{R\to\infty}\lambda(R) = 0 = \lambda_\infty$. On the other hand, for formula (a) $\lambda(R) > 0$ only for $R \in (0, L_v)$ and negative for $R > L_v$. Thus, if R can grow beyond L_v such that $R > L_v$, then $\lim_{R\to\infty}\lambda(R) < 0$. But, we should be able to recover similar results as $R\lambda(R)$ will be negative with solutions to the equation $R'(t) = R\lambda(R)$ attracted to L_v,[2] and a separate analysis would be required. If for (a) we assume that L_v is very large, with initial condition $R_0 \ll L_v$, then we can bound R by L_v but having $\lim_{R\to\infty}\lambda(R) = \lambda_\infty$. The functions defined by formulas (a) and (b) in Eq. (1) have been used in [9,34] for modelling mosquito population dynamics. They are commonly known in the literature respectively as the Verhulst–Pearl logistic [42] and the Maynard-Smith–Slatkin [43] growth models, while (c), known as the Ricker model [44], has been used in fisheries modelling. Unlike the logistic model, (b) and (c) in Eq. (1) are nonlinear and asymptotic to zero for large values of R. Though non-linear, these two functions can be approximated by the logistic growth model by using the value $L_v = -\frac{\lambda_0}{\lambda'(0)}$ in (a) in the case where $\lambda(R)$ is defined by either (b) or (c) in Eq. (1). The Verhulst–Pearl birth rate function is often used because of its linearity and hence mathematical tractability of the resulting equations. In what follows, we shall often not write down a formula for the explicit birth function being used, but we shall assume our birth rate function, whenever it shall be needed, is of a suitable type, indexed by its corresponding carrying capacity L. For the most part in what follows, we will consider that $\lim_{R\to\infty}\lambda(R) = \lambda_\infty = 0$, which means unless otherwise noted as for the case of the logistic model, in which case $\lim_{R\to\infty}\lambda(R) = \lambda_\infty < 0$.

2.1. Modelling repeated feeding

We now extend the model presented in [9] to include multiple feeding attempts. It is common practice as in [9,34] to ignore the effect of male mosquitoes in the modelling framework since our developed model is aimed at investigating "mosquito-human" transmitted diseases as well as mosquito growth dynamics via human interactions, only female mosquitoes that systematically seek and bite humans for blood

[1] The mosquito's blood preference factor defines whether or not the mosquito prefers animal (or non-human) blood over human blood. It is generally accepted that each mosquito has its blood preference factor or zoophilic index, and so for a proper modelling exercise, we must take into consideration this fact and model the parameter K introduced here and shown on Table 2. See Section 2.2(i) of [20] for a discussion and derivation of the parameter K. Note that the units of K is humans obtained as follows: if we let χ_A denote the number of mosquitoes per animal (represented by A) with a preference for animal blood and χ_H the number of mosquitoes per human (represented by H) with a preference for human blood, then a total of $\chi_A A$, respectively, $\chi_H H$ mosquitoes are questing for blood from animals, respectively, humans. Thus $\chi_A A+\chi_H H$ is the total number of questing mosquitoes, with $\frac{\chi_A A}{\chi_A A+\chi_H H}$ the proportion of meals from animals and $\frac{\chi_H H}{\chi_A A+\chi_H H}$ the proportion from humans. Since our focus is on mosquito population growth in light of the human–mosquito interaction and its link to malaria transmission dynamics, and without loss of generality we can assume that $\chi_H > 0$ and define $\varsigma = \frac{\chi_A}{\chi_H}$, so that the fractions of meals that will be taken from humans is $\frac{\chi_H H}{\chi_A A+\chi_H H} = \frac{H}{(\frac{\chi_A}{\chi_H})A+H} = \frac{H}{K+H}$, where $K = \varsigma A$ which has units of humans. Likewise, the fraction of meals taken from animals is $\frac{\chi_A A}{\chi_A A+\chi_H H} = \frac{K}{K+H}$.

[2] The limiting solution for the updated equation $R'(t) = R\lambda(R) - \mu_R R$ can be easily and equally obtained

Table 1
A table showing the different state variables used in this model, their description and quasi-dimensional units. The units are Mosquitoes (M).

State variable	Description of the state variables	Quasi-dimension
B	Density of breeding site mosquitoes. These are newly emerged adult mosquitoes at the breeding site together with all other adult mosquitoes that have returned to the breeding site to lay eggs.	M
Q	Density of questing mosquitoes. These are fertilised adult mosquitoes that have left the breeding site and are questing for blood at the human habitat.	M
R	Density of well blood fed and resting mosquitoes. These are mosquitoes that have successfully harvested a blood meal and are now resting in view of returning to the breeding site to lay eggs.	M
W	Density of waiting class mosquitoes. These are mosquitoes that have attempted, at least once, and failed to feed on humans. They are waiting for the next opportunity to quest again for blood within the human population.	M

Table 2
A table showing the different parameters used in this model, their description and quasi-dimensional units. The units are Humans (H), Mosquito (M) and Time (T).

Parameter	Description of parameters	Quasi-dimension
H	Constant human population and a source of blood for the questing mosquitoes.	H
$K = \frac{\chi_A}{\chi_H} A$	Re-scaled constant that accounts for the availability of an animal or alternative blood source for mosquitoes, whereby $\frac{\chi_H H}{\chi_A A+\chi_H H} = \frac{H}{K+H}$ is the fraction of mosquito meals taken from humans, and $\frac{\chi_A A}{\chi_A A+\chi_H H} = \frac{K}{K+H}$ is the fraction taken from animals. χ_A, respectively χ_H, are the numbers of mosquitoes per animals, respectively humans, with preference for animal, respectively human, blood.	H
a	Flow rate at which female adult mosquitoes of type R return to breeding sites to lay eggs.	T^{-1}
μ_x	Natural death rate of mosquitoes of type x mosquitoes.	T^{-1}
$b^* = b\frac{H}{K+H}$	b is the per capita flow rate at which mosquitoes of type B visit human habitat sites, while b^* gives the weighted rate, weighted by the proportion of blood meals derived from humans.	T^{-1}
$c^* = c\frac{H}{K+H}$	c is the per capita flow rate at which mosquitoes of type W visit human habitat sites in search for a blood meal after they tried and failed, while c^* gives the weighted rate, weighted by the proportion of blood meals derived from humans .	T^{-1}
p	Probability that a questing mosquito successfully harvests a blood meal during a feeding encounter with humans.	1
θ	Probability that a questing mosquito that failed to harvest a blood meal during a feeding encounter survived the encounter	1
τ	Mass action contact parameter between mosquitoes and humans.	$H^{-1}T^{-1}$

are considered. This assumptions is equivalent to stating that we do not explicitly model mosquito mating patterns in the demographic models for mosquito dynamics that we present here. However, we shall assume that questing mosquitoes are also fertilised. In [9], it is assumed that during questing, a mosquito either succeeds with probability p to harvest blood from a human or is killed with probability $1-p$ during the same feeding attempt. That is, in that model, once a mosquito engages the feeding attempt, failure to feed led to certain death of the mosquito. The certain dead assumption linked to failure to feed is too strong a restriction that we now start to relax. It is more realistic to assume that some questing mosquito do survive a failed feeding attempt and that such surviving mosquitoes will, in general, seek to quest again since the previous questing was unsuccessful and the fertilised mosquitoes are driven by a natural reproductive urge to blood feed. We now assume that if questing is unsuccessful, the questing mosquito is either killed, or moved to a waiting class denoted by W. We assume that this process continues till the mosquito dies a natural death, is killed or succeeds in harvesting a blood meal. This process has been summarised in Fig. 1.

The Breeding site mosquitoes. The process starts with breeding site mosquitoes which comprise the newly emerged adult mosquitoes together with any older mosquitoes that have returned to the breeding site to lay eggs. These are denoted by the variable B. So breeding site mosquitoes are increased when new adults emerge at rate $aR\lambda(R)$. Their density also increases when resting mosquitoes of type R return to the breeding site to lay eggs. The density reduces when these breeding site mosquitoes migrate to the human habitats at rate b^* per breeding site mosquito or when they die naturally at rate μ_B per breeding site mosquito. The equation for the rate of change of the type B mosquitoes, as in [9] ignoring delay effects, takes the form

$$\frac{dB}{dt} = \underbrace{aR\lambda(R)}_{(1)} + \underbrace{aR}_{(2)} - \underbrace{(b^* + \mu_B)B}_{(3)}, \tag{2}$$

where a, $b^* = \frac{bH}{K+H}$, μ_B are positive constants as described in Table 2. The term in b^* has two parameters: H the total human population and K a parameter to represent an alternative blood source for the questing mosquitoes. The provenance of K is based on the fact that human-biting mosquitoes frequently also seek and harvest blood from animals and this has an effect on the mosquito control problem and consequently on the transmission of human mosquito borne diseases. As indicated earlier, a detailed description of the parameter K is given in [20]. In Eq. (2), the different terms are explained as follows:

(1) This term models the rate of eclosion of new adult female mosquitoes as a result of eggs laid by mosquitoes of type R. The

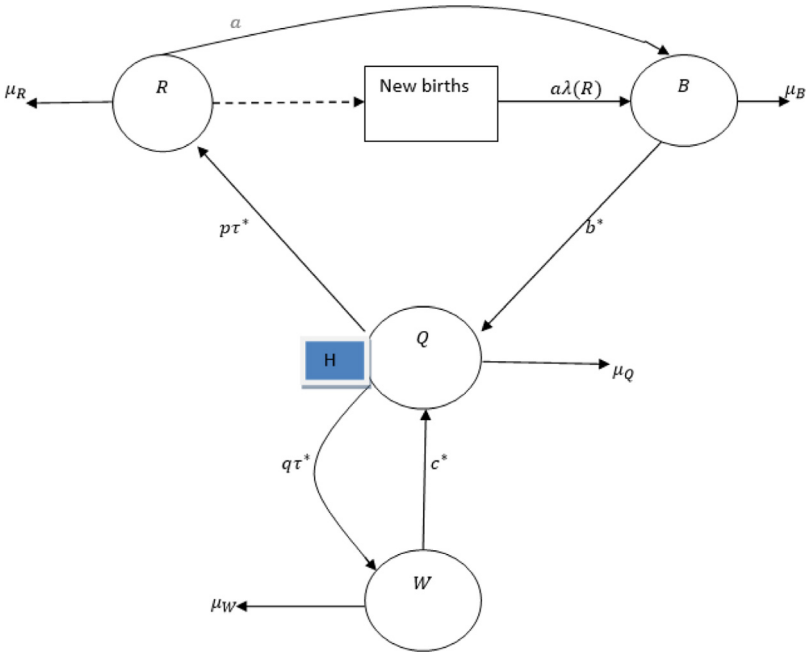

Fig. 1. Extension of the model in [9] to include multiple feeding attempts. The total mosquito population is divided into distinct classes representing vectors at the breeding site, those questing, those resting after a blood meal or those in the waiting class. When type B mosquitoes arrive at the human habitat sites, they become type W mosquitoes. If a type Q mosquito successfully harvests blood, it becomes a type R mosquito. If questing is unsuccessful, the mosquito is either killed or is moved to a waiting class, W. Mosquitoes in the waiting class are attracted back to the human population, where they have another chance to quest and the process continues.

specific form of this term will depend on the type of mosquito under discussion, whether the *Anopheles sp* mosquito, for example, or the *Aedes sp* mosquito, based on their aquatic characteristics [13]. We note this formulation does not explicitly account for the aquatic life stages. Instead the contributions from the aquatic stages to the growth of the adult mosquito population is implicitly embedded via the function $\lambda(R)$.

(2) This term models the rate of return of older mosquitoes to the breeding site to lay eggs.

(3) This term models the rate of removal of the breeding site mosquito either by migration to the human habitat sites at rate b^*B, or by natural death at rate $\mu_B B$.

The Questing mosquitoes. Fertilised mosquitoes, type B mosquitoes from the breeding site, migrate to the human habitat at the indicated rate to become questing mosquitoes, that is, mosquitoes of type Q. The migration is driven by the fact that these mosquitoes require a blood meal for the maturation of their eggs, with blood obtained either from the human or animal population. In this model, we account only for mosquitoes that quest for blood within the human population. At the human habitat site we assume that the mosquitoes quests by making attempts at making contacts and interacting with humans via simple mass action contact. If questing is successful (with probability p), the mosquito becomes well fed and reproducing mosquito of type R. If the questing fails (with probability $1-p$), we assume that a fraction, θ, of these mosquitoes that failed the feeding attempt are moved to the waiting class, W, while the remaining $(1-\theta)$ are killed. Thus the density of mosquitoes in the questing class increases, when the breeding site and waiting class mosquitoes arrive at human habitat site. The density of the questing mosquitoes decreases when they die of natural causes, or if they succeed in feeding to move out of the class into the resting class, or if they fail to feed moving into the waiting class. Assuming a natural death rate μ_Q per Q mosquito, we have the following equation for the rate of change of the density of type Q mosquitoes:

$$\frac{dQ}{dt} = \underbrace{b^*B}_{(1)} - \underbrace{p\tau^*Q}_{(2)} - \underbrace{\theta(1-p)\tau^*Q}_{(3)} - \underbrace{(1-\theta)(1-p)\tau^*Q}_{(4)} - \underbrace{\mu_Q Q}_{(5)} + \underbrace{c^*W}_{(6)} \tag{3}$$

where $\tau^* = \tau H > 0$, p, θ, b^* are positive constants and explained in Table 2. Each of the terms is explained as follows:

(1) New questing mosquitoes from the breeding site.

(2) Questing mosquitoes that survive feeding encounter and successfully acquire blood meal.

(3) Questing mosquitoes that survive feeding encounter but did not acquire blood meal. These live to quest again for the needed blood meal.

(4) Deaths due to questing. These vectors did not survive feeding encounter as they were killed in the process.

(5) Deaths due to natural causes. These vectors die due to natural causes.

(6) Mosquitoes from the waiting class that return to human habitats to again attempt to quest for blood.

The Waiting class mosquitoes. The density of mosquitoes in the waiting class increases when questing mosquitoes fail to take a blood meal and are not killed. The density there decreases when these mosquitoes are attracted back to the human population, where they can quest again for blood. They can also die by natural causes. The equation for the rate of change of the mosquitoes in the waiting class is

$$\frac{dW}{dt} = q\tau^*Q - (c^* + \mu_W)W, \tag{4}$$

where τ^*, $q = \theta(1-p)$, $c^* = \frac{cH}{H+K}$, μ_W are positive constants, as explained in Table 2.

The Resting class mosquitoes. The well fed and resting mosquitoes are simply referred to as the resting mosquitoes. These are generated when questing mosquitoes succeed to blood feed. Their size decreases when they migrate to the breeding site to lay eggs or when they die naturally. The equation governing the rate of change is

$$\frac{dR}{dt} = p\tau^*Q - (a + \mu_R)R, \tag{5}$$

where p, τ^*, μ_R and a are positive constants.

The system of equations modelling the multiple feeding human–mosquito interactive framework is then given by putting together Eqs. (2)–(5), to have

$$\begin{aligned}\frac{dB}{dt} &= aR\lambda(R) + aR - (b^* + \mu_B)B,\\ \frac{dQ}{dt} &= b^*B + c^*W - (\tau^* + \mu_Q)Q,\\ \frac{dW}{dt} &= q\tau^*Q - (c^* + \mu_W)W,\\ \frac{dR}{dt} &= p\tau^*Q - (a + \mu_R)R,\end{aligned} \tag{6}$$

together with an appropriate set of initial conditions. One form of initial data that can be assigned could be

$$B(0) = B_0,\ Q(0) = R(0) = W(0) = 0. \tag{7}$$

In Ngwa et *al.* [37], a procedure for computing the death rates for mosquitoes at each gonotrophic cycle stage, based on the remaining life period of the mosquito, was presented. Here, we have not explicitly counted all the gonotrophic cycles and it is no longer straightforward to give an accurate prediction on the values of the death rates. However, if we assume that the natural death rates of the mosquitoes at each stage is approximately inversely proportional to the remaining life period for the mosquito in question, then we can write down the general prescription

$$\mu_x \approxeq \frac{1}{\text{remaining life period for mosquito of type } x}, \tag{8}$$

where the maximum average remaining life period is the lifespan of the mosquito in question. At the start of the process, mosquitoes of type B are younger than mosquitoes of type R with the ages of the mosquitoes of types Q and W lying in between these two extremes, i.e. $\mu_B \leq \mu_Q \leq \mu_W \leq \mu_R$. As the process progresses, however, mosquitoes at the breeding site are now made up of the newly emerged mosquitoes and those that successfully fed to return to the breeding site and their remaining life is different. In that case the aforementioned inequality is no longer true. However we continue to use this relation for the birth rates for approximation purposes.

2.2. Model's basic properties

Let $\boldsymbol{x} : \mathbb{R}^+ \longrightarrow \mathbb{R}^4$ be the vector valued function such that $\boldsymbol{x}(t) = (B(t), Q(t), W(t), R(t))$. The system (6) can be written in the form

$$\frac{d\boldsymbol{x}}{dt} = \boldsymbol{f}(\boldsymbol{x}),\quad \boldsymbol{x}(0) = \boldsymbol{x}_0, \tag{9}$$

where $\boldsymbol{f} : \mathbb{R}^4 \longrightarrow \mathbb{R}^4$ is a vector valued function defined as: $\boldsymbol{f}(\boldsymbol{x}) = (f_1(\boldsymbol{x}), f_2(\boldsymbol{x}), f_3(\boldsymbol{x}), f_4(\boldsymbol{x}))$, with $f_1(\boldsymbol{x}) = aR\lambda(R) + aR - (b^* + \mu)B$, $f_2(\boldsymbol{x}) = b^*B + c^*W - (\tau^* + \mu)Q$, $f_3(\boldsymbol{x}) = q\tau^*Q - (c^* + \mu)W$ and $f_4(\boldsymbol{x}) = p\tau^*Q - (a + \mu)R$.

Lemma 2.1. *The function $\boldsymbol{f}$ in (9) is Lipschitzian*

Proof. See Appendix A. For more information, see [45]. □

Theorem 2.1 (*Existence, Uniqueness, Positivity and Boundedness of Solutions*)**.** *The differential Eq. (9) has a unique positive solution that is bounded.*

Proof. See Appendix A and also [45] □

2.3. Reparameterisation and scaling

To remove the dimension-like character of the variables in the system given by model (53), we re-scale by considering the change of coordinates:

$$t^* = \frac{t}{T^0},\quad B^* = \frac{B}{B^0},\quad Q^* = \frac{Q}{Q^0},\quad W^* = \frac{W}{W^0},\quad R^* = \frac{R}{R^0} \tag{10}$$

where

$$\begin{aligned}T^0 &= \frac{1}{a + \mu_R},\quad R^0 = L,\quad Q^0 = \frac{R^0(a + \mu_R)}{p\tau^*} = \frac{(a + \mu_R)L}{p\tau^*},\\ W^0 &= \frac{q\tau^*Q^0}{c^* + \mu_W} = \left(\frac{q}{c^* + \mu_W}\right)\left(\frac{L(a + \mu_R)}{p}\right),\\ B^0 &= \frac{Q^0(\tau^* + \mu_Q)}{b^*} = \frac{(a + \mu_R)(\mu_Q + \tau^*)L}{p\tau^*b^*}.\end{aligned} \tag{11}$$

Dropping the asterisks we have the scaled system

$$\begin{aligned}\frac{dB}{dt} &= \alpha R\lambda(R) + \alpha R - \rho B,\\ \frac{dQ}{dt} &= \gamma(B + \beta W - Q),\\ \frac{dW}{dt} &= \delta(Q - W)\\ \frac{dR}{dt} &= Q - R,\end{aligned} \tag{12}$$

where it is understood that we have scaled the corresponding form in the birth rate function $\lambda(U)$, and

$$\alpha = \frac{aR^0T^0}{B^0} = \left(\frac{a}{a + \mu_R}\right)\left(\frac{b^* + \mu_B}{a + \mu_R}\right)\left(\frac{b^*}{b^* + \mu_B}\right)\left(\frac{\tau^*}{\tau^* + \mu_Q}\right)p < \left(\frac{b^* + \mu_B}{a + \mu_R}\right) = \rho, \tag{13}$$

$$\beta = = \frac{c^*W^0}{Q^0(\tau^* + \mu_Q)} = q\left(\frac{c^*}{c^* + \mu_W}\right)\left(\frac{\tau^*}{\tau^* + \mu_Q}\right) < 1, \tag{14}$$

$$\gamma = \frac{\mu_Q + \tau^*}{a + \mu_R},\qquad \delta = \frac{c^* + \mu_W}{a + \mu_R}. \tag{15}$$

We can recover the model, without a waiting class, studied in [9] from (12) by setting[3] $\beta = \delta = 0$. In what follows we characterise how allowing these terms to be non-zero affect the results in [9]. Based on the fact that mosquitoes start from a breeding site and end up at the same breeding site $b = a$. We deduce that $b^* < a$, since b^* is b weighted by $\frac{H}{H+K}$, with the two equal if $K = 0$. For $K \neq 0$ and based on the assumption that $\mu_B \leq \mu_R$ we must have $\rho < 1$. Thus we have that $0 \leq \beta < 1$, $0 \leq \alpha < \rho < 1$, $0 < \gamma < \infty$. The parameter γ can therefore be useful in studying the ensuing dynamics since it is linked to the mass action parameter $\tau^* = \tau H$ that measures the availability of blood meals for the mosquitoes. Similarly, the parameters β and δ, which are also linked to the mass action parameter τH and the rate of return to the questing state, c^*, will play an important role in the ensuing analysis. We note that c^* can be very small if it takes long for the waiting class vectors to return to the questing state (that is $\frac{1}{c^*}$ is very large) or c^* can be very large if the waiting time to return to quest is very short (that is $\frac{1}{c^*}$ is very small). So to be general, all we can say about the relative size of the parameter δ is that $0 < \delta < \infty$. These reparameterisations clearly show how the parameters α, β and ρ compare with unity as well as how ρ compares with α.

3. Mathematical analysis

In this section we present a mathematical development of the derived model. In the process we will determine the essential properties of the system. We start with the issue of existence and stability of steady constant solutions.

3.1. Existence and stability of steady state solutions

In this subsection, we shall investigate the existence and linear stability of steady state solutions for the scaled system.

Theorem 3.1 (*Existence of Steady States Solutions.*)**.** *Let $\lambda : [0, \infty) \longrightarrow \mathbb{R}$ be a continuously differentiable strictly monotone decreasing function with $\lambda(0+) = \lambda(0) > 0$ satisfying A1 − A3. System (12) has at least two steady state solutions: The trivial steady state $(0, 0, 0, 0)$ which always exists*

[3] From the formulation, setting $c^* = 0$, $\mu_W = 0$ and $\theta = 0$ which corresponds to $q = 0$, with zero initial values for $W(t)$ yields the system with $W(t) = 0\ \forall t \geq 0$ and we can recover the simplified model as desired.

and at least one non-trivial steady state solutions represented in terms of R^* *as* $(B^*, Q^*, W^*, R^*) = (B^*(R^*), Q^*(R^*), W^*(R^*), R^*)$, *where* $R^* = \lambda^{-1}\left(\frac{\rho(1-\beta)}{\alpha} - 1\right)$, *which exists if*

$$\lim_{R\to\infty} \lambda(R) < \frac{\rho(1-\beta)}{\alpha} - 1 < \lambda(0). \tag{16}$$

Proof. We start by noting that whenever $\frac{\rho(1-\beta)}{\alpha} - 1$ lies between $\lambda(0)$ and $\lim_{R\to\infty}\lambda(R)$, then inequality (16) follows by the strict monotonicity of the function λ. If $E = (B^*, Q^*, W^*, R^*)$ is a steady state (equilibrium solution) of system (12), it must satisfy

$$\alpha R^*\lambda(R^*) + \alpha R^* - \rho B^* = \gamma(B^* + \beta W^* - Q^*) = \delta(Q^* - W^*) = Q^* - R^* = 0. \tag{17}$$

From the last two equations of (17), we have that $Q^* = W^* = R^*$. From the first equation, we have $B^* = \frac{\alpha R^*(\lambda(R^*)+1)}{\rho}$ and so substituting in the second equation yields the equation $R^*\left(\frac{\alpha(\lambda(R^*)+1)}{\rho} + \beta - 1\right) = 0$. The solution $R^* = 0$ gives the trivial steady state which always exist. The non-trivial steady state, whenever it exists, is determined from the equation $\frac{\alpha(\lambda(R^*)+1)}{\rho} + \beta - 1 = 0$, which can be rewritten as $\lambda(R) = \frac{\rho(1-\beta)}{\alpha} - 1$. Since λ is strictly monotone decreasing and continuous, with $\lambda(0) > \lim_{R\to\infty}\lambda(R)$, whenever $\left(\frac{\rho(1-\beta)}{\alpha} - 1\right)$ lies between $\lambda_\infty = \lim_{R\to\infty}\lambda(R)$ and $\lambda(0)$, there exists $R^* > 0$ such that $\lambda(R^*) = \frac{\rho(1-\beta)}{\alpha} - 1$, by the intermediate value theorem. Since λ is monotone decreasing, the constructed R^* exists and its value is uniquely given by the formula $R^* = \lambda^{-1}\left(\frac{\rho(1-\beta)}{\alpha} - 1\right)$ whenever $\lambda_\infty < \frac{\rho(1-\beta)}{\alpha} - 1 < \lambda(0)$ as required. □

Theorem 3.1 assures us that the system can have up two steady state solutions as follows:

(*a*) The trivial steady state $E_0 : (B^*, Q^*, W^*, R^*) = (0, 0, 0)$ (18)

(*b*) The non-trivial steady state

$$E_1 : (B^*, Q^*, W^*, R^*) = (B^*(R^*), R^*, R^*, R^*) \tag{19}$$

where $R^* = \lambda^{-1}\left(\frac{\rho(1-\beta)}{\alpha} - 1\right)$ whenever inequality (16) holds. We can then gather considerable information about the size of the parameter β by examining left side of the inequality Eq. (16) in details as we do in Remark 3.1.

Remark 3.1. We note that for the class of models considered here for which $\lim_{R\to\infty}\lambda(R) > 0$, the inequality (16) implies that $\frac{\rho(1-\beta)}{\alpha} > 1$, which then translates to the inequality $0 \le \beta < \frac{\rho-\alpha}{\rho}$ to satisfy the bound on β from Eq. (14); namely, $\beta < 1$. This places a stricter bound on the values of β. For models for which $\lambda(R)$ can go negative, $\lambda(R) < 0$ can be interpreted as the case of a decline in the breeding site mosquitoes, with the restriction on β, namely, $0 \le \beta < \frac{\rho-\alpha}{\rho}$, no longer true. In that case, the region $\beta < \frac{\rho-\alpha}{\rho} < 1$, would then be plausible, extending the interval to $0 \le \beta < 1$ as earlier derived in Eq. (14). In the commentaries that follow, since our discussion is based on a general model, we will continue to use the restricted interval $0 \le \beta < \frac{\rho-\alpha}{\rho}$, unless otherwise noted.

Remark 3.2. We can also gather considerable information about the system by examining the inequality (16) in details as follows:

1. The whole of the inequality (16), for any suitable λ, provides a necessary condition for the existence of a non-trivial steady state solution to our problem.
2. The right half of the inequality in (16) given by $\frac{\rho(1-\beta)}{\alpha} - 1 < \lambda(0)$ can be rearranged, in two ways, to give two threshold parameters as follows:
   (a) In the first instance, we have $\frac{\rho(1-\beta)}{\alpha} - 1 < \lambda(0) \Rightarrow \mathcal{N}_1 > 1$, where
   $$\mathcal{N}_1 = \frac{\alpha\lambda(0)}{\rho(1-\beta) - \alpha}. \tag{20}$$
   In this case, for non-negative $\mathcal{N}_1$, we require a restriction on β given by $0 \le \beta < \frac{\rho-\alpha}{\rho}$.
   (b) In the second instance, we have $\frac{\rho(1-\beta)}{\alpha} - 1 < \lambda(0) \Rightarrow \mathcal{N}_2 > 1$, where
   $$\mathcal{N}_2 = \frac{\rho\beta + \alpha\lambda(0)}{\rho - \alpha}, \tag{21}$$
   which is always non-negative for all non-negative values of the constituent parameters, since $\alpha < \rho$, and there is no restriction on β.
3. Any one of the threshold parameters $\mathcal{N}_1$ and $\mathcal{N}_2$ so identified by (20) and (21) can be useful in determining further properties of the model, including the stability of steady state solutions, provided we find a useful interpretation for it in the context of the model presented here.

Though the natures of $\mathcal{N}_1$ and $\mathcal{N}_2$ appear different, both exhibit threshold like properties as expressed in the following results:

Theorem 3.2 (*a*). $\mathcal{N}_1 > 1 \Leftrightarrow \mathcal{N}_2 > 1$, *(b)* $\mathcal{N}_1 \le 1 \Leftrightarrow \mathcal{N}_2 \le 1$

Proof. (a) Suppose $\mathcal{N}_1 > 1 \Rightarrow \frac{\alpha\lambda(0)}{\rho(1-\beta)-\alpha} > 1 \Rightarrow \alpha\lambda(0) > \rho(1-\beta) - \alpha \Rightarrow \frac{\beta\rho+\alpha\lambda(0)}{\rho-\alpha} = \mathcal{N}_2 > 1$. On the other hand suppose $N_2 > 1 \Rightarrow \frac{\beta\rho+\alpha\lambda(0)}{\rho-\alpha} > 1 \Rightarrow \frac{\alpha\lambda(0)}{\rho(1-\beta)-\alpha} = \mathcal{N}_1 > 1$. (b) is just the contrapositive of (a). □

Theorem 3.3. *Let the conditions of Remark 3.1 and the result of Theorem 3.2 continue to hold. Let* $\mathcal{N}$ *be any of the quantities* $\mathcal{N}_1$ *or* $\mathcal{N}_2$. *Then, we have the following:*

1. *(i) Whenever* $\mathcal{N} < 1$, *then* $\mathcal{N}_1 < \mathcal{N}_2$, *(ii) Whenever* $\mathcal{N} > 1$, *then* $\mathcal{N}_1 > \mathcal{N}_2$, *and (iii)* $\mathcal{N}_1 = 1 \Leftrightarrow \mathcal{N}_2 = 1$.
2. *When* $\beta = 0$, $\mathcal{N}_1 = \mathcal{N}_2 = \frac{\alpha\lambda(0)}{\rho-\alpha} = \mathcal{R}_m$.

Proof. 1.(*i*) Suppose $\mathcal{N} < 1$. Then by Theorem 3.2, both $\mathcal{N}_1 < 1$ and $\mathcal{N}_2 < 1$. $\mathcal{N}_1 < 1 \Rightarrow \frac{\alpha\lambda(0)-(\rho(1-\beta)-\alpha)}{\rho(1-\beta)-\alpha} < 0$. Now, $\mathcal{N}_1 - \mathcal{N}_2 = \frac{\rho\beta(\alpha\lambda(0)-(\rho(1-\beta)-\alpha))}{(\rho(1-\beta)-\alpha)(\rho-\alpha)} < 0$. So $\mathcal{N}_1 < \mathcal{N}_2$. 1.(*ii*) is established similarly. 1.(*iii*) Suppose $\mathcal{N}_1 = 1$, then $\alpha\lambda(0) = (\rho(1-\beta) - \alpha)$. Substitute this value of $\alpha\lambda(0)$ in $\mathcal{N}_2$ to see results. Similar argument if we start with $\mathcal{N}_2 = 1$. The result in 2. follows from substituting $\beta = 0$ in $\mathcal{N}$. □

Fig. 2 illustrates the results of Theorems 3.2 and 3.3

Stability of steady state solutions

To explore the stability properties of the steady states of this model, we note that the community or Jacobian matrix corresponding to model (16) is given by

$$A(R^*) = \begin{pmatrix} -\rho & 0 & 0 & \alpha H(R^*) \\ \gamma & -\gamma & \beta\gamma & 0 \\ 0 & \delta & -\delta & 0 \\ 0 & 1 & 0 & -1 \end{pmatrix} \tag{22}$$

where $H(R^*) = 1 + \lambda(R^*) + R^*\lambda'(R^*)$ and R^* is any of the steady state solutions described by Theorem 3.1. Here, we study the local stability properties of the steady state solutions by examining the eigenvalues of the Jacobian matrix, $A(R^*)$, evaluated at the steady state. If we denote by ζ the eigenvalues of $A(R^*)$, then ζ satisfies

$$|A(R^*) - \zeta I| = 0 \iff (\rho+\zeta)(1+\zeta)\big((\gamma+\zeta)(\delta+\zeta) - \beta\delta\gamma\big) - \gamma\alpha\beta H(R^*)(\delta+\zeta) = 0. \tag{23}$$

This is a fourth degree polynomial in ζ which we write in the form

$$P_4(\zeta) = \zeta^4 + a_3\zeta^3 + a_2\zeta^2 + a_1\zeta + a_0 \tag{24}$$

where

$$\begin{aligned} a_3 &= \delta + \gamma + \rho + 1, \quad a_2 = \rho + \gamma\delta(1-\beta) + (\gamma+\delta)(1+\rho), \\ a_1 &= \delta\gamma(1-\beta)(1+\rho) + \rho(\delta+\gamma) - \gamma\alpha H(R^*), \\ a_0 &= \delta\gamma\rho(1-\beta) - \delta\gamma\alpha H(R^*), \end{aligned}$$

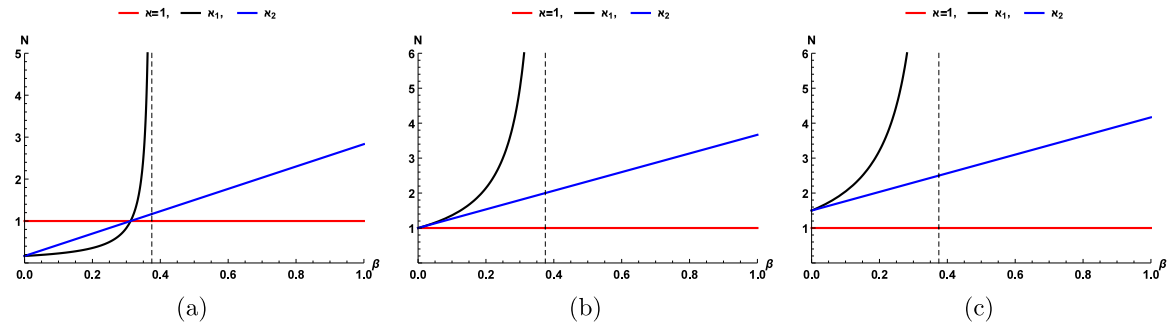

Fig. 2. Illustration of Theorems 3.2 and 3.3. The two threshold parameters $\mathcal{N}_1$ and $\mathcal{N}_2$, plotted as a function of β for $\alpha = 0.5$ and $\rho = 0.8$, fixed, and for $\lambda(0) = 0.1$ (graph (a)), $\lambda(0) = 0.6$ (graph (b)) and $\lambda(0) = 0.9$ (graph (c)). As β approaches its maximum value $\frac{\rho-\alpha}{\rho}$, illustrated by the dashed vertical line, $\mathcal{N}_1$, represented by the black curve grows unbounded, while $\mathcal{N}_2$, represented by the green curve, remains bounded. Both are compared with the value 1, the red line, showing that they are always both less than unity or both larger then unity. The $\mathcal{N}-$ intercept corresponds to the value of $\mathcal{R}_m = \frac{\alpha\lambda(0)}{\rho-\alpha}$, when $\beta = 0$. Thus, mathematically, both threshold parameters can be used as a measure for the basic offspring number. Biologically one may be more suitable than the other.

and we have completely characterised the coefficients of the polynomial in terms of the parameters of the system showing us clearly that only a_1 and a_0 will change as a function of the steady state's value. The next result shows the instability of the trivial steady state when any one of the Threshold parameters, $\mathcal{N}_1$ or $\mathcal{N}_2$ is greater than unity.

Theorem 3.4. *Let $\lambda : [0,\infty) \to \mathbb{R}$ be positive and monotone decreasing. Let us denote by $\mathcal{N}$ any one of the threshold parameters identified by (20) and (21). Then $\mathcal{N} > 0$ determines the stability properties of the trivial steady state in the sense that when $0 < \mathcal{N} < 1$, the trivial steady state is locally-asymptotically stable and unstable if $\mathcal{N} > 1$.*

Proof. Clearly, referring to the coefficients of (24) when evaluated at $R^* = 0$, we have $a_3 > 0$, $a_2 > 0$ since $1 > \beta$. We rewrite a_1 and a_0 in terms of the threshold parameter, $\mathcal{N}$ as follows:

$$a_1 = \begin{cases} \gamma\left(\rho\beta + (1-\beta)\delta(\rho+1) + (1-\mathcal{N})(\rho(1-\beta)-\alpha)\right) + \delta\rho & \text{if} \quad \mathcal{N} = \mathcal{N}_1, \\ \gamma\left((1-\beta)\delta(\rho+1) + \beta\rho + (\rho-\alpha)(1-\mathcal{N})\right) + \delta\rho & \text{if} \quad \mathcal{N} = \mathcal{N}_2. \end{cases}$$

$$a_0 = \begin{cases} \alpha\delta\gamma(\rho(1-\beta)-\alpha)(1-\mathcal{N}) & \text{if} \quad \mathcal{N} = \mathcal{N}_1, \\ \alpha\delta\gamma(\rho-\alpha)(1-\mathcal{N}) & \text{if} \quad \mathcal{N} = \mathcal{N}_2. \end{cases}$$

Here, $\mathcal{N}_1$ and $\mathcal{N}_2$ are as defined by (20) and (21). We then note that $a_1 > 0$ whenever $\mathcal{N} < 1$. Also a_0 is strictly greater than zero whenever $0 < \mathcal{N} < 1$. The local stability of the trivial steady state when $0 < \mathcal{N} < 1$ follows immediately from the Routh–Hurwitz conditions, [46], while its instability for $\mathcal{N} > 1$ can be seen by observing that as $\mathcal{N}$ increase through $\mathcal{N} = 1$ to values where $\mathcal{N} > 1$, a_0 changes sign from positive to negative. Thus, by Descartes rule of signs, there is a positive real root for ζ indicating the presence of exponentially growing solutions in the linear regime. □

The result of Theorem 3.4 seems to indicate that only local stability for the trivial steady state might be plausible when $\mathcal{N} < 1$. The next result shows that we do in fact have global stability in these circumstances.

Theorem 3.5. *Suppose λ satisfy the conditions in Theorem 3.4. The trivial steady state, $\mathbf{0} = (0,0,0,0)$ of model (12) is globally and asymptotically stable in $\mathbb{R}^4_+$ whenever $\mathcal{N} \le 1$.*

Proof. Let $T_m = B + Q + W + R$ be the total vector population. Then $T_m \le \frac{\alpha\lambda_m}{\mu}$, where λ_m and μ are as given in Theorem A.3 and its proof. Define

$$\Omega = \{(B,Q,W,R) \in \mathbb{R}^4_+ : 0 \le T_m \le \frac{\alpha\lambda_m}{\mu}\}, \tag{25}$$

then Ω is a positively invariant subset of $\mathbb{R}^4_+$. Next, we construct the function

$$\mathcal{L}(\boldsymbol{x}) = A_v B + \frac{\rho}{\gamma}A_v Q + \frac{\beta\rho}{\delta}A_v W + \rho(1-\beta)A_v R, \tag{26}$$

for $\boldsymbol{x} = (B,Q,W,R) \in \Omega$ and any positive constant A_v. It is clear that $\mathcal{L}(0,0,0,0) = 0$ and $\mathcal{L}(\boldsymbol{x}) > 0$ for all $\boldsymbol{x} \in \Omega\backslash\{\mathbf{0}\}$ since $\beta < 1$. The function $\mathcal{L}$ so defined is therefore a Lyapunov function of system (12). Since the right hand side of system (12) is made up of continuously differentiable functions, for each $\boldsymbol{x} \in \mathbb{R}^4_+$ the Lyapunov derivative is

$$\begin{aligned} \frac{d\mathcal{L}(\boldsymbol{x})}{dt} &= \left(\frac{\partial\mathcal{L}}{\partial B}, \frac{\partial\mathcal{L}}{\partial Q}, \frac{\partial\mathcal{L}}{\partial W}, \frac{\partial\mathcal{L}}{\partial R}\right) \cdot \left(\frac{dB}{dt}, \frac{dQ}{dt}, \frac{dW}{dt}, \frac{dR}{dt}\right), \\ &= A_v\frac{dB}{dt} + \frac{\rho}{\gamma}A_v\frac{dQ}{dt} + \frac{\beta\rho}{\delta}A_v\frac{dW}{dt} + \rho(1-\beta)A_v\frac{dR}{dt}, \\ &= \mathcal{L}_0 A_v R(\mathcal{N}-1) + \alpha R\left(\lambda(R) - \lambda(0)\right)A_v, \\ &\quad \mathcal{L}_0 = \begin{cases} (\rho(1-\beta)-\alpha) & \text{if} \quad \mathcal{N} = \mathcal{N}_1, \\ (\rho-\alpha) & \text{if} \quad \mathcal{N} = \mathcal{N}_2, \end{cases} \\ &= \mathcal{L}_0 A_v R(\mathcal{N}-1) + \alpha R^2\left(\lambda'(\tilde{R})\right)A_v, \\ &\quad \tilde{R} \in (0,R) \text{ a mean value point.} \end{aligned}$$

We note that $\mathcal{L}_0$ so defined is positive for $\mathcal{N} > 0$ since $\alpha < \rho$ and $\mathcal{N}_1 > 0$ whenever $\beta < \frac{\rho-\alpha}{\rho}$. Then, $\frac{d\mathcal{L}(\boldsymbol{x})}{dt} < 0 \ \forall\ \boldsymbol{x} \in \Omega\backslash\{\mathbf{0}\}$ whenever $0 < \mathcal{N} \le 1$ since λ is monotonically decreasing and $\mathcal{L}_0 > 0$. Since $\frac{d\mathcal{L}(\boldsymbol{x})}{dt} < 0$ for all $\boldsymbol{x} \in \Omega\backslash\{\mathbf{0}\}$, the Lyapunov–LaSalle theorem [47] assures us that all paths in $\Omega\setminus\{\mathbf{0}\}$ approach the largest positively invariant subset $\tilde{\Omega} \subset \Omega$ wherein $\frac{d\mathcal{L}(\boldsymbol{x})}{dt} = 0$. $\tilde{\Omega}$ is the singleton $\{\boldsymbol{x} = \mathbf{0}\}$. Hence $\boldsymbol{x} \to \mathbf{0}$ as $t \to \infty$ whenever $\mathcal{N} \le 1$ and so the global stability for $\mathbf{0}$ whenever $\mathcal{N} \le 1$ is established. □

The result in 3.5 indicate that mosquito extinction is possible. In Appendix B, we present some detail results on the stability properties of the non-trivial steady state. There, we demonstrate the existence of a Hopf bifurcation to periodic solutions by deriving expressions for the initial amplitude and phase of oscillating solutions.

3.2. The basic offspring number

We have been carrying the two threshold parameters identified by (20) or (21) which guarantee the existence of positive steady state solutions for the system in our analyses. In this subsection, we discuss in depth the nature of the parameter $\mathcal{N}$ and its derivation. We start by introducing the notion of a *gonotrophic cycle path* and then demonstrate that the form of the parameter $\mathcal{N}$ is dependent on how we view the flow and transitions on the gonotrophic cycle path

Mosquitoes of type B visit vertebrate host such as humans at vertebrate habitat sites (questing places) to become questing mosquitoes of type Q which eventually become resting mosquitoes of type R if they successfully acquire a blood meal. If the mosquitoes of type R survive the resting period they eventually return to the breeding site and lay eggs that hatch to produce new adult mosquitoes. There is therefore a reproductive path, the gonotrophic cycle path, that the female adult mosquito must follow through out its reproductive life.

Definition 3.1 (*Gonotrophic Cycle Path.*)**.** A gonotrophic cycle path way is the directed path traced by the mosquito as it moves though a connected lattice that has vertices or nodes at breeding sites, questing places and resting locations. A female mosquito is said to have completed a gonotrophic cycle if it successfully migrates from a breeding site to a vertebrate host, takes blood, rests and then migrates back to a breeding site and lays eggs.

Breeding sites, questing places and resting locations need not be distinct for each individual mosquito. However, a gonotrophic cycle is called complete[4] if that path constitutes a cycle that starts at a breeding site and ends at a breeding site accompanied by a successful laying of eggs at the breeding site. As the female *Anopheles sp* mosquito completes several gonotrophic cycles during its entire reproductive life, there is a flow of biomass from generation to generation through the blood feeding habit of the mosquito. That is, each mosquito that survives the gonotrophic cycle will introduce new offspring into the adult mosquito pool, and the mosquito population can continue to grow only in those circumstances where each adult female mosquito can generate, on average, more than one descendant mosquito into the adult mosquito pool upon completion of all its gonotrophic cycles. Obviously each adult mosquito that falls out of the gonotrophic cycle path way (by, for example, failing to blood feed or being killed during the resting phase) will not contribute to the next generation of adult mosquitoes. This leads us to consider the concept of a *basic offspring number*. The following definition was used in [3]:

Definition 3.2 (*Basic Offspring Number.*)**.** The basic offspring number is the average number of new adult mosquitoes, that arise from one adult female reproducing mosquito during its entire period of reproductivity.

The basic offspring number is a threshold parameter comparable with the basic reproduction number in epidemiology, and has the same interpretation in that if this number is larger than one, we expect the mosquito population to thrive and if it is less than one we expect the mosquito population to die out over time.

We can identify the basic offspring number with a threshold quantity, which is an aggregate of parameters of the system. Such an aggregate parameter can be identified in several ways: (1) It can be seen as a parameter that sets conditions for the existence of a non-trivial steady state solution for the system under consideration. This we have analysed with Remark 3.2 and seen that such a threshold parameter is not uniquely determined. (2) It can also be seen as a parameter whose size determines the stability or instability of the trivial steady state as we have seen in the result of Theorem 3.4. Now, with the hope to finding a plausible reason to select a suitable threshold parameter for our model, we borrow a leaf from epidemiological concepts and use, as a third method, the next generation matrix method of van den Driessche and Watmough [48], to calculate the basic offspring number as the largest eigenvalue of a positive linear operator. To do this, we consider as before $\boldsymbol{x} = (B, Q, W, R)^T$ a column vector in $\mathbb{R}^4$ and write the system $\boldsymbol{x}'(t) = \boldsymbol{f}(\boldsymbol{x}(t))$ as a difference of two vectors $\mathcal{F}$ and $\mathcal{V}$ such that $\boldsymbol{f}(\boldsymbol{x}) = \mathcal{F}(\boldsymbol{x}) - \mathcal{V}(\boldsymbol{x})$, where $\mathcal{F}$ is a vector of new adult mosquitoes and $\mathcal{V}$ is a vector of transitions into the different stages. If $\mathcal{N}$ is this basic offspring number, then $\mathcal{N} = \max_\lambda\{\lambda : \lambda \text{ is an eigenvalue of } FN^{-1}\}$ where F and N are respectively the Jacobian matrices of $\mathcal{F}$ and $\mathcal{V}$ evaluated at the trivial state $B = Q = W = R = 0$.

[4] In [37], an example of a mathematical model for mosquito population dynamics that explicitly undertakes complete gonotrophic cycle counts is analysed. To understand the flow, we must separate the events that occur at the nodes or vertices of the path (laying of eggs at the breeding site, blood feeding at the questing places, egg maturation at the resting locations) from the path itself; even though successful occurrence of each of the events at the respective nodes, is crucial in the realisation or completion of the gonotrophic cycle.

The computation of the next generation matrix requires that we interpret very clearly what we mean by *new births* in the system, as well as *transitions*. It has been reported that the choice of interpretation of the two concepts "new births" and "transition" can have an effect on the outcome in the sense that it can lead to different threshold values that differ in size but retain their threshold-like character [49–51]. In the original model studied in [9], there was no ambiguity in the interpretation of new births into the system and transitions in that system. With the introduction of the waiting class W, here, there is then a possibility of regarding mosquitoes in the W class as being out of the main flow (or gonotrophic cycle path) and can be seen as "new births" when they return to the main flow path. This opens up a different possibility for describing the next generation matrix. Thus the generation and transition of new mosquitoes onto the gonotrophic cycle path is affected by the introduction of the waiting class W, giving us two possible next generation matrices as we now present below:

On the one hand, we can define

$$\mathcal{F}_1(\boldsymbol{x}) = \begin{pmatrix} \alpha R\lambda(R) \\ 0 \\ 0 \\ 0 \end{pmatrix}, \quad \mathcal{V}_1(\boldsymbol{x}) = \begin{pmatrix} \rho B - \alpha R \\ \gamma(Q - B - \beta W) \\ \delta(W - Q) \\ R - Q \end{pmatrix}. \tag{27}$$

In this characterisation, we assume that "new births", i.e. new mosquitoes onto the gonotrophic cycle path constitute the new adult mosquitoes that emerge into the system at the breeding site and all other terms in the system are seen as transitions (change of state from breeding site to questing, waiting to quest and resting). Thus all other stages in the process are regarded as demographic transition shifts. This interpretation leads to a next generation matrix M_1 given by

$$M_1 = F_1 V_1^{-1} = \begin{pmatrix} -\frac{\alpha\lambda(0)}{\alpha+(\beta-1)\rho} & -\frac{\alpha\rho\lambda(0)}{\gamma(\alpha+(\beta-1)\rho)} & -\frac{\alpha\beta\rho\lambda(0)}{\delta(\alpha+(\beta-1)\rho)} & \frac{\alpha(\beta-1)\rho\lambda(0)}{\alpha+(\beta-1)\rho} \\ 0 & 0 & 0 & 0 \\ 0 & 0 & 0 & 0 \\ 0 & 0 & 0 & 0 \end{pmatrix} \tag{28}$$

The basic offspring number $\mathcal{N}_1$ is thus the dominant eigenvalue of M_1 and is given by

$$\begin{aligned} \mathcal{N}_1 &= \max_\lambda\{\lambda : \lambda \text{ is an eigenvalue of } M_1\} \\ &= -\frac{\alpha\lambda(0)}{\alpha + (\beta-1)\rho} = \frac{\alpha\lambda(0)}{\rho(1-\beta) - \alpha}, \end{aligned} \tag{29}$$

which is the expression in (20), and is non-negative only for $0 \le \beta < \frac{\rho-\alpha}{\rho}$. The basic offspring number so derived shows a strong dependence on the values of α and $\lambda(0)$ as was reported in [9], in that when either $\alpha = 0$ or $\lambda(0) = 0$, its value is zero. It also shows strong dependence on the size of β in the sense that as β approaches its upper bound $\frac{\rho-\alpha}{\rho}$, $\mathcal{N}_1$ can become very large for fixed values of α and $\lambda(0)$ (see Fig. 2). Biologically, this seems to be in error since the mosquitoes have not yet completed a gonotrophic cycle and we do not expect the reproductive ability of the insects to increase as such only as a function of β. There seems therefore to be a poor interpretation of transition events and births using this scenario.

On the other hand. we can define

$$\mathcal{F}_2(\boldsymbol{x}) = \begin{pmatrix} \alpha R\lambda(R) \\ \gamma\beta W \\ 0 \\ 0 \end{pmatrix}, \quad \mathcal{V}_2(\boldsymbol{x}) = \begin{pmatrix} \rho B - \alpha R \\ \gamma(Q - B) \\ \delta(W - Q) \\ R - Q \end{pmatrix}. \tag{30}$$

In this second case, we assume that once a mosquito enters the W class from the questing Q class, they have actually fallen out of the gonotrophic cycle path and can be considered as new births events when it returns to the gonotrophic cycle path by rejoining the W class. If the mosquitoes that fail to feed were allowed to return to the breeding site, the Q class will coincide with the B class and this type of consideration will not be possible. Since mosquitoes from several

sources that fail to feed, even those that initially went to quest for blood meals in animal population can enter this waiting class, we are permitted to interpreted flows from the Q class into the W class as new births to write down the splitting represented by $\mathcal{F}_2$ and $\mathcal{V}_2$ indicated in (30). This then leads to the next generation matrix M_2, given by

$$M_2 = F_2 V_2^{-1} = \begin{pmatrix} -\frac{\alpha\lambda(0)}{\alpha-\rho} & -\frac{\alpha\rho\lambda(0)}{\gamma(\alpha-\rho)} & 0 & \frac{\alpha\rho\lambda(0)}{\rho-\alpha} \\ \frac{\beta\gamma}{\rho-\alpha} & -\frac{\beta\rho}{\alpha-\rho} & \frac{\beta\gamma}{\delta} & \frac{\alpha\beta\gamma}{\rho-\alpha} \\ 0 & 0 & 0 & 0 \\ 0 & 0 & 0 & 0 \end{pmatrix}. \tag{31}$$

The basic offspring number $\mathcal{N}_2$ is thus the dominant eigenvalue of M_2 and is given by

$$\mathcal{N}_2 = \max_{\lambda}\{\lambda : \lambda \text{ is an eigenvalue of } M_2\} = -\frac{\alpha\lambda(0)+\beta\rho}{\alpha-\rho} = \frac{\beta\rho+\alpha\lambda(0)}{\rho-\alpha}, \tag{32}$$

which is the expression in (21) and it is always non-negative since $0 < \rho - \alpha$. The second basic offspring number so derived still shows a strong dependence on α as was seen before but when $\alpha = 0$, its value is no longer zero, capturing the fact that there are still mosquitoes in the waiting class that can join the cycle. The second threshold value so computed appears to have more desirable properties in that it clearly shows the contributions from the mosquitoes from the gonotrophic cycle path that bypass the W class, $\frac{\alpha\lambda(0)}{\rho-\alpha}$, and contributions from those on the path that comes from the W class, $\frac{\beta\rho}{\rho-\alpha}$. Since the original model, studied in [9], was based on the gonotrophic cycle pathway towards population growth as is followed by a fertilised mosquito, we may therefore interpret "new births" and "transitions" to mean that these events take place on that very gonotrophic cycle path that is followed by each fertilised adult female mosquito. Biologically, we conclude that the alternate interpretation of "new births" and "transitions", that led to formula (32), has given a threshold parameter that captures the expected behaviour and is a generalisation from the value computed when $\beta = 0$ studied in [9].

Each of the decompositions given by (27) and (30) is such that the right hand side $\boldsymbol{f}(\boldsymbol{x})$ can be decomposed into the form $\boldsymbol{f}(\boldsymbol{x}) = \mathcal{F}_i(\boldsymbol{x}) - \mathcal{V}_i(\boldsymbol{x})$ where $\mathcal{F}_i$ is interpreted as a vector of new adult mosquitoes and $\mathcal{V}_i$ is a vector of transitions into the different stages for $i = 1, 2$. It is straightforward to establish that each of the given decomposition satisfies the condition outlined in [48]; the two threshold parameters so described are mathematically useful as threshold parameters, as established by the proof of Theorem 3.2.

Remark 3.3.

1. We remark that the expressions for $\mathcal{N}_1$ and $\mathcal{N}_2$ first identified in Eqs. (20) and (21) were initially obtained as threshold parameters associated with the existence of the non trivial steady state and the instability of the trivial steady state, before the next generation approach was utilised. In particular, both $\mathcal{N}_1$ and $\mathcal{N}_2$ are associated with the inequality $\frac{\rho(1-\beta)}{\alpha} - 1 < \lambda(0)$ shown in Eq. (16). One rearrangement of the inequality yields the expression for $\mathcal{N}_1$ with the condition $\mathcal{N}_1 = \frac{\alpha\lambda(0)}{\rho(1-\beta)-\alpha} > 1$, while a second rearrangement yields expression for $\mathcal{N}_2$ with the condition $\mathcal{N}_2 = \frac{\rho\beta+\alpha\lambda(0)}{\rho-\alpha} > 1$, both necessary conditions for the instability of the trivial steady state as well as the existence of the non-trivial steady state. Furthermore, the third method was via the next generation approach, in which we considered the "new births" via breeding site mosquitoes that complete the gonotrophic cycle pathway and returned to the breeding site to lay their first batch of eggs. Specifically, at the onset of the dynamics, some mosquitoes may fail to obtain blood and join the W class mosquitoes, eventually returning to quest, succeeding before returning to the breeding site to lay their first batch of eggs. These mosquitoes had fallen out of the gonotrophic cycle pathway (but had not completed their first gonotrophic cycle), eventually to return to complete their gonotrophic cycle a little later than those breeding site mosquitoes that succeeded during their initial quest attempt. Thus, we believe that accounting for them in this way, as part of the new births terms, is legitimate and yields the expression $\mathcal{N}_2$. Without accounting for those mosquitoes that eventually rejoined the gonotrophic cycle pathway after the initial delay, we then get the expression as in $\mathcal{N}_1$.
2. From a biological point of view, $\mathcal{N}_1$ and $\mathcal{N}_2$ have different interpretations. Firstly, $\mathcal{N}_1 = \frac{\alpha\lambda(0)}{\rho(1-\beta)-\alpha}$, can be interpreted as the fraction of mosquitoes that returned to the breeding site to lay eggs without ever leaving the gonotrophic cycle pathway. These mosquitoes succeeded in their first attempt. On the other hand, $\mathcal{N}_2 = \frac{\rho\beta+\alpha\lambda(0)}{\rho-\alpha} = \frac{\rho\beta}{\rho-\alpha} + \frac{\alpha\lambda(0)}{\rho-\alpha}$, adds those mosquitoes that returned to the breeding site to lay eggs after succeeding on their first attempt $\left(\frac{\alpha\lambda(0)}{\rho-\alpha}\right)$, to those that failed but succeeded at a later time to eventually complete their cycle and return to the breeding site $\left(\frac{\rho\beta}{\rho-\alpha}\right)$.
3. We believe that our methodology is quite robust in that three different procedures led to the two expressions for $\mathcal{N}_1$ and $\mathcal{N}_2$, with the next generation approach illustrating how these two expressions are associated to two different interpretations of "new births" and "transitions". We believe this is a novelty in our work and incites a discussion on how we view and compute the next generation matrices as well as how we use such threshold parameters as a predictive quantity. Here, as a threshold parameter, there is no ambiguity in that $\mathcal{N}_1 > 1 \iff \mathcal{N}_2 > 1$.

4. Multiple feeding and its effects on mosquito population dynamics

Here, we further explore the effects of inclusion of the multiple feeding attempts affects the dynamics of the mosquito populations as derived in this paper. We begin by summarising the model and results for the case where the W class is absent as studied in [9].

4.1. Special case where the W-compartment is absent

We can regain the model in [9] from (17) by setting $\beta = \delta = 0$ in (12). In this case, we have

$$\begin{aligned} \frac{dB}{dt} &= \alpha R\lambda(R) + \alpha R - \rho B, \\ \frac{dQ}{dt} &= \gamma(B - Q), \\ \frac{dR}{dt} &= Q - R, \end{aligned} \tag{33}$$

$$B(0) = B_0, \quad Q(0) = Q_0, \quad R(0) = R_0.$$

The system (33) has been studied in detail [9,34]. Results such as the existence of a threshold parameter

$$\mathcal{R}_m = \frac{\alpha\lambda(0)}{\rho-\alpha}, \tag{34}$$

that determines the stability properties of the trivial steady state, as well as the existence and stability of nontrivial steady state solutions were proven in [34]. In [9], it was also shown that there exists a parameter regime for which the system (33) admits a Hopf Bifurcation, as has been demonstrated for the model here in Appendix B, and that the amplitude of oscillations of the ensuing dynamics at the Hopf bifurcation point can be constructed using a perturbation analysis. It is also known that stability properties of the bifurcating solutions at the Hopf bifurcation point can be approximated using a centre manifold theory, [52]. Although, in general, computation of the centre manifold is not always possible, it is always possible to approximate the centre manifold to any degree of accuracy by a function of class C^2 [53];

this we illustrate in Appendix C. For now, we recall simply that the threshold parameter, $\mathcal{R}_m$, defined in (34), determines the stability properties of the zero steady state and existence of the nontrivial steady state as follows:

1. Global and asymptomatic stability of the trivial steady state when $\mathcal{R}_m \leq 1$.
2. Instability of the trivial steady state whenever $\mathcal{R}_m > 1$ which is accompanied with the birth of a second steady state, the non-trivial steady state, when $\mathcal{R}_m$ increases through the value $\mathcal{R}_m = 1$ to values where $\mathcal{R}_m > 1$.
3. Stability of the non-trivial steady state for $1 < \mathcal{R}_m < \mathcal{R}_m^c$.
4. Occurrence of a Hopf bifurcation at $\mathcal{R}_m = \mathcal{R}_m^c > 1$ and the emergence of stable limit cycle solutions as $\mathcal{R}_m$ further increases from $\mathcal{R}_m^c$. The value of $\mathcal{R}_m^c$, being completely determined by the parameters of the system.

Details on these results can be found in [9,10,34].

4.2. Effects of the W compartment on the mosquito dynamics

In [9], questing can either be successful with probability p or unsuccessful with probability $1 - p$. If unsuccessful, the mosquito is assumed killed. Here, we have relaxed the certain death scenario for the questing mosquitoes in Section 2 by introducing a waiting class of mosquitoes, W, from where mosquitoes that did not succeed to feed, and did not die in the course of the feeding attempt, can be attracted back to the human habitat where they are given another opportunity to quest. With this additional class of mosquitoes, we have been able to establish the existence of a threshold parameter $\mathcal{N}$ defined as one of Eqs. (20) or (21) that determines the stability properties of the zero steady state and the existence of the nontrivial steady state. In particular, we have established that:

1. The threshold parameter that determined the properties of solutions of the system is no longer unique, which differs from the results of the model without the W (waiting) compartment.
2. The trivial steady state solution, which always exists for all parameter values is globally and asymptotically stable whenever $0 \leq \mathcal{N} \leq 1$ and unstable when $\mathcal{N} > 1$ as was the case with the model without the W-compartment.
3. A nontrivial steady state, which exists only for parameter values for which $\mathcal{N} > 1$, can be stable for a range of parameter values but can also be driven to instability via a Hopf bifurcation for certain values of the parameters of the system. In fact this result has the same character as with the model without the W-compartment
4. The effect of the W class shows itself from the provisions of Remark 3.1 that if $\frac{\rho-\alpha}{\rho} \leq \beta < 1$, and we also insist that the birthrate function λ is such that $\lambda : [0,\infty) \to [0,\infty)$, then we cannot have a non-zero steady state. That is, so long as the birth rate function is non-negative, we can have a nontrivial steady state only for values of β such that $\beta < \frac{\rho-\alpha}{\rho} < 1$.

There are therefore restrictions and attributes of the system that come about as a result of the re-interpretation of the dynamics of interaction of the mosquitoes with humans to include ability to attempt to feed at multiple times. We now examine carefully the effect of the W component on the mosquito dynamics taking in turn each of the characteristic attributes of the system. In particular we examine what happens if we allow the existence of a more general function λ such that $\lambda : [0,\infty) \to \mathbb{R}$, so that $\lambda(R)$ can be negative for some values of R, as would be the case with the logistic growth function. Our answers will further illustrate the necessity to properly interpret the meaning of $\lambda(R)$. For example, if we interpret $\lambda(R)$ as the birth rate function per mosquito of type R, then a negative value of λ will only signify that the population B, whose growth rate is determined by the sign of λ, will be experiencing decreasing growth.

4.2.1. On the threshold parameters and their sizes

We compare the two threshold parameters given by Eqs. (20) and (21) with the corresponding value when $\beta = 0$ as given in (34). We begin with a discussion on how, for example, β compares with ρ and α. To do so, we let

$$\nu = 1 - \frac{\alpha}{\rho} \text{ and set } \beta = s\nu, \tag{35}$$

and note that $0 < \nu \leq 1$ since $0 \leq \alpha < \rho$. Thus $0 < s\nu \leq s$ which yields $0 < \beta \leq s$. Then, from the restriction on β, for which $\mathcal{N}_1 > 0$ (so that $0 \leq \beta \leq \frac{\rho-\alpha}{\rho}$), we can only allow s to fall in the range $0 \leq s < 1$. Then it becomes clear that using the characterisation (35) for s and ν, we have

$$\mathcal{N}_1 = \frac{\alpha\lambda(0)}{\rho(1-\beta)-\alpha} = \frac{\mathcal{R}_m(\rho-\alpha)}{\rho(1-\beta)-\alpha} = \frac{\mathcal{R}_m}{1-s}, \quad 0 \leq s < 1, \tag{36}$$

and

$$\mathcal{N}_2 = \frac{\alpha\lambda(0)+\rho\beta}{\rho-\alpha} = \frac{\mathcal{R}_m(\rho-\alpha)+\rho\beta}{\rho-\alpha} = \mathcal{R}_m + s, \quad 0 \leq s < 1, \tag{37}$$

So even though $\mathcal{N}_1$ and $\mathcal{N}_2$ have the threshold like character as proved by Theorem 3.2, $\mathcal{N}_1$ seems to over estimate the threshold parameter when seen as a function of s. In particular, $\lim_{s\to 1^-} \mathcal{N}_1 = +\infty$ while $\lim_{s\to 1^-} \mathcal{N}_2 = \mathcal{R}_m + 1$. That the parameter $\mathcal{N}_1$ given by (36) is larger when compared with $\mathcal{N}_2$ given by (37) becomes evident if we recognise $\frac{1}{1-s}$ as the limit of an infinite geometric series, so that

$$\mathcal{N}_1 = \mathcal{R}_m(1 + s + s^2 + s^3 + s^4 + \cdots).$$

That $\mathcal{N}_1$ diverges to infinity as $s \to 1^-$ captures the fact that some of the W mosquitoes can have a very long lifespan pushing up the value of the threshold number indefinitely. So, if we view the dynamics of the mosquito in the lens of the threshold parameter $\mathcal{N}_2$, the restriction $s < 1$ is not needed. In this case, the relation $s \geq 1$ yields $\nu s \geq \nu$. That is, $\nu \leq \nu s = \beta < 1$. This gives us the possibility $\frac{\rho-\alpha}{\rho} \leq \beta < 1$. For this set of values of β, $\mathcal{N}_1$ is negative and is no longer useful as a threshold parameter, while $\mathcal{N}_2$ is still useful as a threshold parameter. It would appear therefore, that $\mathcal{N}_2$ is a better threshold parameter to consider over $\mathcal{N}_1$, and that a more realistic restriction on the size of the parameter β is given by the inequality $0 \leq \beta < 1$.

The appearance of two possible threshold parameters make us realise that the interpretation of what a transition is, in the context of compartmental models, has a profound effect on the actual dynamics of the system.

4.2.2. On the survivability of the mosquito population

In Theorem 3.4, we proved the local stability of the trivial steady state when $0 < \mathcal{N} < 1$, with the stronger condition of global stability proved in Theorem 3.5 for $0 < \mathcal{N} \leq 1$, tied to the extinction of the mosquito population. From Eqs. (36) and (37), $\mathcal{N} = \mathcal{N}_1$ and $\mathcal{N} = \mathcal{N}_2$ are both bigger than $\mathcal{R}_m$, the threshold estimate when $\beta = 0$, indicating that the waiting class has a stabilising effect of the chances of survival for the mosquito population. So, some of the mosquitoes that survive the questing attempt do indeed eventually succeed to increase the chances of survival of the insect. When $\beta = 0$, $\mathcal{N}_1 = \mathcal{N}_2$ and both reduce to the threshold parameter for the model without repeated feeding attempts, namely $\mathcal{R}_m = \frac{\alpha\lambda(0)}{\rho-\alpha}$. When $0 < \mathcal{N} < 1 \Rightarrow \mathcal{R}_m < 1$, but the converse is not necessarily true. The next result shows that there is a choice of β for which any of $\mathcal{N}_1$ or $\mathcal{N}_2$ can be bigger than one when $\mathcal{R}_m < 1$.

Theorem 4.1. *Let $\mathcal{R}_m < 1$, then there is a choice of β in the allowable range of values of β for which $\mathcal{N} > 1$.*

Proof. Let $\mathcal{R}_m = \frac{\alpha\lambda(0)}{\rho-\alpha} < 1$. Assume without loss of generality that for some $\varepsilon > 0$, with $0 < \varepsilon < 1$, $\frac{\alpha\lambda(0)}{\rho-\alpha} = 1 - \varepsilon$. So $\alpha\lambda(0) = (\rho-\alpha)(1-\varepsilon)$.

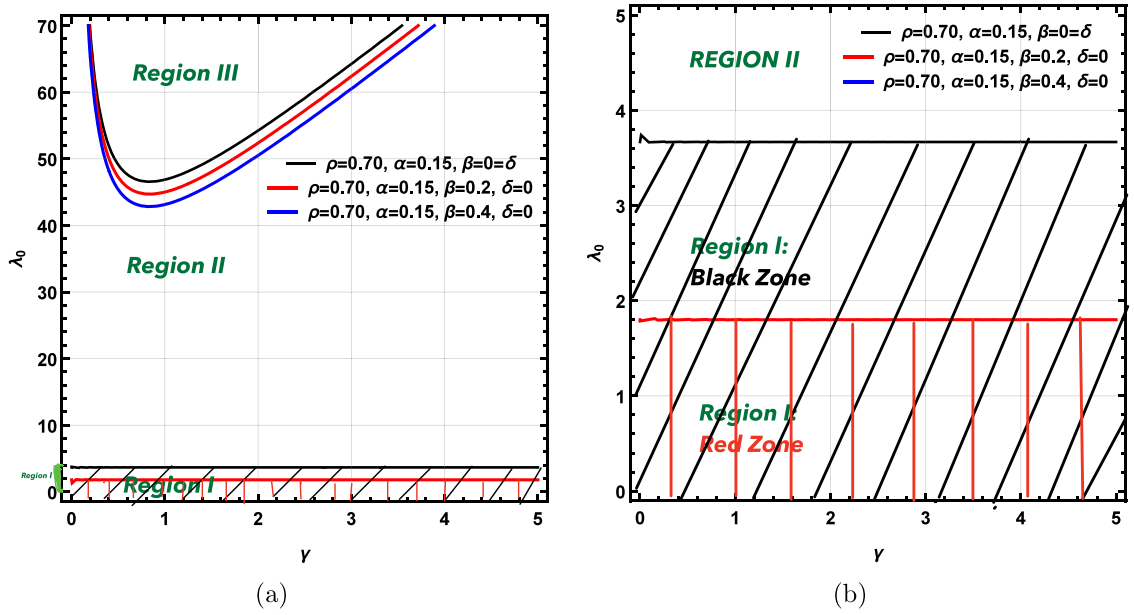

Fig. 3. Illustration of Theorem 4.1 for $\alpha = 0.15$, $\rho = 0.70$ and $\delta = 0$, and three β values: 0, 0.2 and 0.4. In the figures, $\lambda_0 = \lambda(0)$. Starting with Fig. 3(a), there are three regions: *Region I* where $\mathcal{N} \leq 1$ and where the trivial steady state exists and is globally stable (see Theorems 3.4, 3.5); *Region II* where $\mathcal{N} > 1$ and $\xi < 1$, where the non-trivial steady state exists and is linearly stable (see Theorem B.1 and Remark B.1), and *Region III* where $\mathcal{N} > 1$ and $\xi > 1$, where the non-trivial steady state exists but loses its stability as it bifurcates to periodic solutions, entering the oscillatory region (see Theorem B.3 and Remark B.2). Fig. 3(b) is a zoom-out of the shaded region in Fig. 3(a), where $\lambda_0 < 4$. As β increases from 0, the region where the trivial steady state exists and is globally stable ($\mathcal{N} \leq 1$), represented by the shaded regions labelled region I, reduces further with increasing β. The region shown by the black shaded zone which is the region when $\beta = 0$ reduces as β increases to 0.2. For the region between $\lambda_0 = 1.8$ and about 3.6, $\mathcal{N} > 1$. As we increase β further to 0.4 we see that *Region I* disappears and the extinction equilibrium no longer exists; there is always a thriving mosquito population which can be driven to a Hopf bifurcation.

Then consider the inequality $\mathcal{N}_1 > 1$. That is $\frac{\alpha\lambda(0)}{\rho(1-\beta)-\alpha} > 1 \Rightarrow \frac{(\rho-\alpha)(1-\varepsilon)}{\rho(1-\beta)-\alpha} > 1 \Rightarrow \frac{\rho-\alpha}{\rho}\varepsilon < \beta < \frac{\rho-\alpha}{\rho}$. The same inequality can be derived using the threshold parameter $\mathcal{N}_2$. □

Theorem 4.1 shows that the waiting class destabilises the trivial steady state. Thus the fact that much energy is required to suppress mosquito population is captured in the model with multiple feeding attempts. The source of this effect can be investigated as follows: From $0 \leq s < 1$, we have $0 \leq s\nu < \nu$ which yields $0 \leq \beta < \nu = \frac{\rho-\alpha}{\rho}$ placing a restriction on the maximum size of β. Even with the restriction on β, we still see that we now have several possibilities that can be seen as pathways towards an increase in the value of the threshold parameter $\mathcal{N}$. When $\beta = \delta = 0$, we had interpreted an increase in $\mathcal{R}_m$ as an increase in $\lambda(0)$. This choice of interpretation was fairly natural given that $\alpha < \rho < 1$ are pretty much fixed parameters of the system. When $\beta > 0$, the size of the threshold parameter can now also be increased by increasing β. There is thus more variability in the outcome of events with the consideration of the waiting class mosquitoes.

Thus the effect of a non-zero β in the model is significant in the sense that it can enhance the existence of non-trivial solutions. This result is illustrated in Fig. 3. The figure also depicts results from Theorems 3.4, 3.5, B.1 and B.3 and Remarks B.1 and B.2.

4.2.3. On the existence of and size of the non-trivial steady state

The steady states of the system are characterised by the results of Theorem 3.1. In particular we require that inequality (16) should hold. For $\beta = 0$, since $\rho > \alpha$, there is one uniquely determined steady state value because of the monotonicity of λ. As β increases from 0, the value of the scaled steady state solution approaches the point $R^* = 1$, which will correspond to the system approaching levels where $\lambda(R) = 0$. This corresponds to the point where $\beta = \frac{\rho-\alpha}{\rho}$.

For models for which $\lambda(R)$ can go negative as in the logistic model, there is a possibility for a second steady state for $\frac{\rho-\alpha}{\rho} < \beta < 1$ that will exists for all values of the parameters and its value is larger than 1. To see this, consider the logistic model where $\lambda(R) = \lambda(0)(1-R)$ which gives the steady state solution $R^* = 1 - \frac{\rho(1-\beta)-\alpha}{\alpha\lambda(0)}$. Suppose $\beta = \frac{\rho-\alpha}{\rho} + \varepsilon$, with $\varepsilon < \frac{\alpha}{\rho}$, then $R^* = 1 + \frac{\rho\varepsilon}{\alpha\lambda(0)}$ which will exist for all values of the parameters and its value is bigger than unity whenever the perturbation $\varepsilon > 0$. For this parameter regime, we expect that since $\lambda(R) < 0$, the rate of production of new eggs is declining and we expect the system to be witnessing decreasing breeding site mosquito populations.

The second point we note about the effect of the W class on the existence of the steady state is on the size of the breeding site mosquitoes, B^*, at equilibrium. From Eq. (17), we see that the $B^* = (1-\beta)R^*$ showing that as β increases from zero towards values near 1, B^* becomes progressively small. So, to sustain the population of the breeding site mosquitoes at equilibrium, the value of β must not be too close to the number one.[5]

In the case where $\beta < \frac{\rho-\alpha}{\rho} < 1$, and while using the logistic growth function, set $\lambda(x) = \lambda(0)(1-x)$ which gives $\lambda^{-1}(x) = 1 - \frac{x}{\lambda(0)}$ which then yields the steady state solution $R^* = W^* = Q^* = \lambda^{-1}\left(\frac{1}{\alpha}\rho(1-\beta) - 1\right) = 1 - \frac{\rho(1-\beta)-\alpha}{\alpha\lambda(0)}$, $B^* = (1-\beta)R^*$, and so we have

$$R^* = \frac{\mathcal{R}_m - 1}{\mathcal{R}_m} + \frac{s}{\mathcal{R}_m} = \frac{\mathcal{N}-1}{\mathcal{N}} \text{ if } \mathcal{N} = \mathcal{N}_1 \text{ or } R^* = \frac{\mathcal{N}-1}{\mathcal{N}-s} \text{ if } \mathcal{N} = \mathcal{N}_2. \tag{38}$$

Therefore, while the steady state values for R and W type mosquitoes are increased because of the consideration of the fact that not all mosquitoes that fail to quest die, the steady state value of the breeding site mosquitoes B is actually reduced. Thus the model without the waiting class overestimates the equilibrium density of mosquitoes at the breeding site. It seems therefore that concentrating control effort on

[5] We defer to a different occasion the discussion on whether or not the fact that for $\frac{\rho-\alpha}{\rho} < \beta < 1$, $\mathcal{N}_1$ as computed by (20) becomes negative gives us a reason to conclude that this particular parameter scenario may not be biologically realistic. For now, given that we are primarily interested in models for which $\lambda(R) > 0$, we shall only note the existence of steady state solutions for which $R^* > 1$, which arises as a result of the assumption that β can be in the range $\frac{\rho-\alpha}{\rho} < \beta < 1$, as a mathematical artifact.

mosquitoes that have left the breeding site will have greater impact on the mosquito population control as more mosquitoes at the equilibrium would be reached. In fact pushing β close to unity will be equivalent to reducing the breeding site population density at equilibrium.

4.2.4. On the size of the instability window

To understand the effect of the waiting class on the instability window, we once more employ the logistic function as an example and note that in this case, the steady state, in the case where $\beta < \frac{\rho-\alpha}{\rho}$, is given by Eq. (38) and then the coefficients of the characteristic polynomial, Eq. (24), become

$$\left.\begin{array}{rcl} a_3 & = & \delta+\gamma+\rho+1, \quad a_2=(\delta+\gamma)(1+\rho)+\delta\gamma(1-\beta)+\rho, \\ a_1 & = & P_0+N_0(\mathcal{N}-1), \quad a_0=\delta N_0(\mathcal{N}-1) \end{array}\right\} \tag{39}$$

$$P_0 = \gamma\rho\beta+\rho\delta+\gamma\delta(1+\rho)(1-\beta), \; N_0 = \begin{cases} \gamma(\rho(1-\beta)-\alpha) & \text{if} \quad \mathcal{N}=\mathcal{N}_1 \\ \gamma(\rho-\alpha) & \text{if} \quad \mathcal{N}=\mathcal{N}_2 \end{cases} \tag{40}$$

When $\beta = \delta = 0$, the characteristic polynomial at the non-zero steady becomes simply $\zeta(\zeta^3 + a_3\zeta^2 + a_2\zeta + a_1) = 0$ and we recover the polynomial studied in [9], which was shown to admit a Hopf bifurcation at the point in parameter space where $a_1 = a_3a_2$, which translates in terms of the threshold parameter to the critical value $\mathcal{N}_c = 1 + \frac{a_3a_2}{\gamma(\rho-\alpha)}$. So, as the threshold parameter increases from 1, the system loses stability at $\mathcal{N}_c$ with the emergence of growing oscillations. In the current case where $\beta \neq 0$ and $\delta \neq 0$, the Hopf bifurcation occurs at that point in the parameter space where $\xi = 1$ as defined by Eq. (56) in Appendix B (Since stability is guaranteed when $0 < \xi < 1$). This translates into the inequality $\frac{a_1}{a_3}\left(a_2 - \frac{a_1}{a_3}\right) - a_0 > 0$, giving rise to an inequality to define the instability window, which we can write in terms of the threshold parameter $\mathcal{N}$ in the form

$$\frac{P_0+N_0(\mathcal{N}-1)}{a_3}\left(a_2-\frac{P_0+N_0(\mathcal{N}-1)}{a_3}\right)-\delta N_0(\mathcal{N}-1)>0. \tag{41}$$

Recall from the parameterisation and parameter groupings given by Eqs. (39) and (40) that when $\beta = \delta = 0$, $P_0 = 0$ and $\mathcal{N}_1 = \mathcal{N}_2 = \mathcal{R}_m$ and inequality (41) collapses to the inequality

$$\frac{N_0(\mathcal{N}-1)}{a_3}\left(a_2-\frac{N_0(\mathcal{N}-1)}{a_3}\right)>0 \Rightarrow 1<\mathcal{N}=\mathcal{R}_m<1+\frac{a_3a_2}{N_0}=1+\frac{a_3a_2}{\gamma(\rho-\alpha)} \tag{42}$$

and we recapture the stability window for the original system. As δ and β increase from zero, the linear character is lost and the quadratic, Eq. (41), promises the existence of an interval $(\mathcal{N}_-, \mathcal{N}_+)$ such that $\mathcal{N}_- < \mathcal{N} - 1 < \mathcal{N}_+$ within which we can expect linear stability. The bounds $\mathcal{N}_-$ and $\mathcal{N}_+$ are simply obtained by regarding Eq. (41) as an equality and solving for $\mathcal{N} - 1$. The new instability window so identified will actually lead to meaningful solutions for those values of the parameters for which $\mathcal{N} > 1$. The instability window now depends on the parameters δ and β in the sense that the system is linearly stable to small perturbations whenever $\mathcal{N}_- < \mathcal{N} - 1 < \mathcal{N}_+$, where

$$\mathcal{N}_-(\delta,\beta) = -\frac{a_3\left(\sqrt{4\delta P_0+(a_2-\delta a_3)^2}+\delta a_3-a_2\right)+2P_0}{2N_0}, \tag{43}$$

$$\mathcal{N}_+(\delta,\beta) = \frac{a_3\left(\sqrt{4\delta P_0+(a_2-\delta a_3)^2}-\delta a_3+a_2\right)-2P_0}{2N_0}. \tag{44}$$

From the size of the parameters, $\mathcal{N}_-(\delta, \beta)$ is always negative and so the region of stability in this case is $0 \leq \mathcal{N} - 1 < \mathcal{N}_+(\delta, \beta)$ where $\mathcal{N}_+(\delta, \beta)$ is given by Eq. (44). We can actually estimate the contributions of the parameters β and δ by noting that

$$\mathcal{N}_+(\delta,\beta) = \mathcal{N}_+(0,0) + \mathcal{N}_+^{\delta}\delta + \mathcal{N}_+^{\beta}\beta + O(\delta\beta), \tag{45}$$

where

$$\mathcal{N}_+^{\delta} = \frac{\partial\mathcal{N}_+(0,0)}{\partial\delta}, \quad \mathcal{N}_+^{\beta} = \frac{\partial\mathcal{N}_+(0,0)}{\partial\beta}, \tag{46}$$

and $\mathcal{N}_+(0, 0)$ is the value of the threshold parameter when $\delta = \beta = 0$ given by the last term in the inequality (42). Evaluation of these partial derivatives shows that $\mathcal{N}_+^{\delta}$ is zero while $\mathcal{N}_+^{\beta}$ is non-zero signifying relative contributions to the size of the stability window when β and δ are both small. The fact that δ captures instead the overall strength of the interactions (see the position of δ on the W equation in system (12)) is thus seen in these initial responses. Now, as β and δ increase from zero, the stability window is affected giving us more room for flexibility and richer dynamics. Note that in the case where $\frac{\rho-\alpha}{\rho} < \beta < 1$, the analysis as we have presented above still holds, except for the fact that $\mathcal{N} = \mathcal{N}_2$ all the way.

We illustrate the effects of the waiting times on the instability window (described by IW) graphically in Figs. 4–9, by plotting the function

$$IW = \delta N_0(\mathcal{N}-1) - \frac{P_0+N_0(\mathcal{N}-1)}{a_3}\left(a_2-\frac{P_0+N_0(\mathcal{N}-1)}{a_3}\right), \tag{47}$$

on the $\gamma - \lambda_0$ plane, the $\gamma - \beta$ plane and the $\gamma - \delta$ plane. Here and in the graphical representations, we will represent $\lambda(0)$ by λ_0. For each of these figures, $\alpha = 0.1$ and $\rho = 0.6$, fixed, while all other parameters are varied, one at a time. Notice that here, the main focus are the waiting parameters, thus these choices. We begin by plotting IW in $3D$ as well as the corresponding level-curve $IW = 0$, both on the $\gamma - \lambda_0$ plane. Clearly, as illustrated in Fig. 4, the size of the instability window increases for positive values of β and δ, with the right arm of the plot of $IW = 0$ becoming flatter. The increase is slight with β alone, as was evident in Fig. 3 as well, but increases significantly for larger values of δ.

Next, we plot IW in $3D$ on the $\gamma - \beta$ plane, together with the corresponding level-curve $IW = 0$. See Figs. 5–6. These figures illustrate a different dynamics in the increase of the instability region in the $\gamma - \beta$ plane. The right arm grows but at a decreasing rate. Additionally, for larger $\lambda(0) = \lambda_0$ values, the level curves can go negative indicating that there are values of γ in which we are always within the oscillatory region. In the illustrated example, Figs. 6(a) and 6(b), γ is roughly between 0.5 and 3.

We next illustrate how the size of the instability window changes in the $\gamma - \delta$ plane as β increases from 0.3 to 0.5 and to 0.8, and for two values of $\lambda(0) = \lambda_0 \in \{50, 90\}$ fixed, with $\alpha = 0.1$ and $\rho = 0.6$, fixed (See Figs. 7–9). For $\lambda_0 = 50$, an increase in β from 0.3 leads to an increase in the oscillatory region, with a significant increase in width for larger β values, allowing for a larger γ window under which oscillatory dynamics are obtained (compare Figs. 7(a) and 7(b) where $\beta = 0.3$ and $\lambda_0 = 50$, to Figs. 8(a) and 8(b) where $\beta = 0.5$, λ_0 unchanged at 50 and to Figs. 9(a) and 9(b) where $\beta = 0.8$, λ_0 unchanged at 50.) If we now increase λ_0 to 90, then the increase in size of the window is two dimensional, with the size increase in width and height allowing for both a larger γ window and wider δ region under which oscillatory dynamics can be obtained (compare Figs. 7(c) and 7(d) where $\beta = 0.3$ and $\lambda_0 = 90$, to Figs. 8(c) and 8(d) where $\beta = 0.5$, λ_0 unchanged at 90 and to Figs. 9(c) and 9(d) where $\beta = 0.8$, λ_0 unchanged at 50.)

4.2.5. On the size of the initial period of oscillations at the bifurcation point

We have established Appendix B that the system can be driven to instability via a Hopf bifurcation as the threshold parameter increases from unity. The initial period of the oscillation is given by Eq. (63). At the bifurcation point, we have that the initial period is $\frac{2\pi}{\omega}$, where we can regard ω as a function of β and δ, to write

$$\omega(\beta,\delta) = \sqrt{\frac{a_1(\beta,\delta)}{a_3(\beta,\delta)}} = \sqrt{\frac{P_0+N_0\mathcal{N}_+(\delta,\beta)}{a_3(\beta,\delta)}}. \tag{48}$$

Observe that $\omega(\beta, \delta) > \omega(0, 0) = \sqrt{a_2(0)} = \sqrt{\rho+\gamma+\rho\gamma}$ obtained by inserting $\delta = 0$ in the value for a_2 in Eq. (39). Therefore the initial period of oscillation in the upgraded system is smaller, capturing a higher frequency of behaviour of the questing mosquitoes.

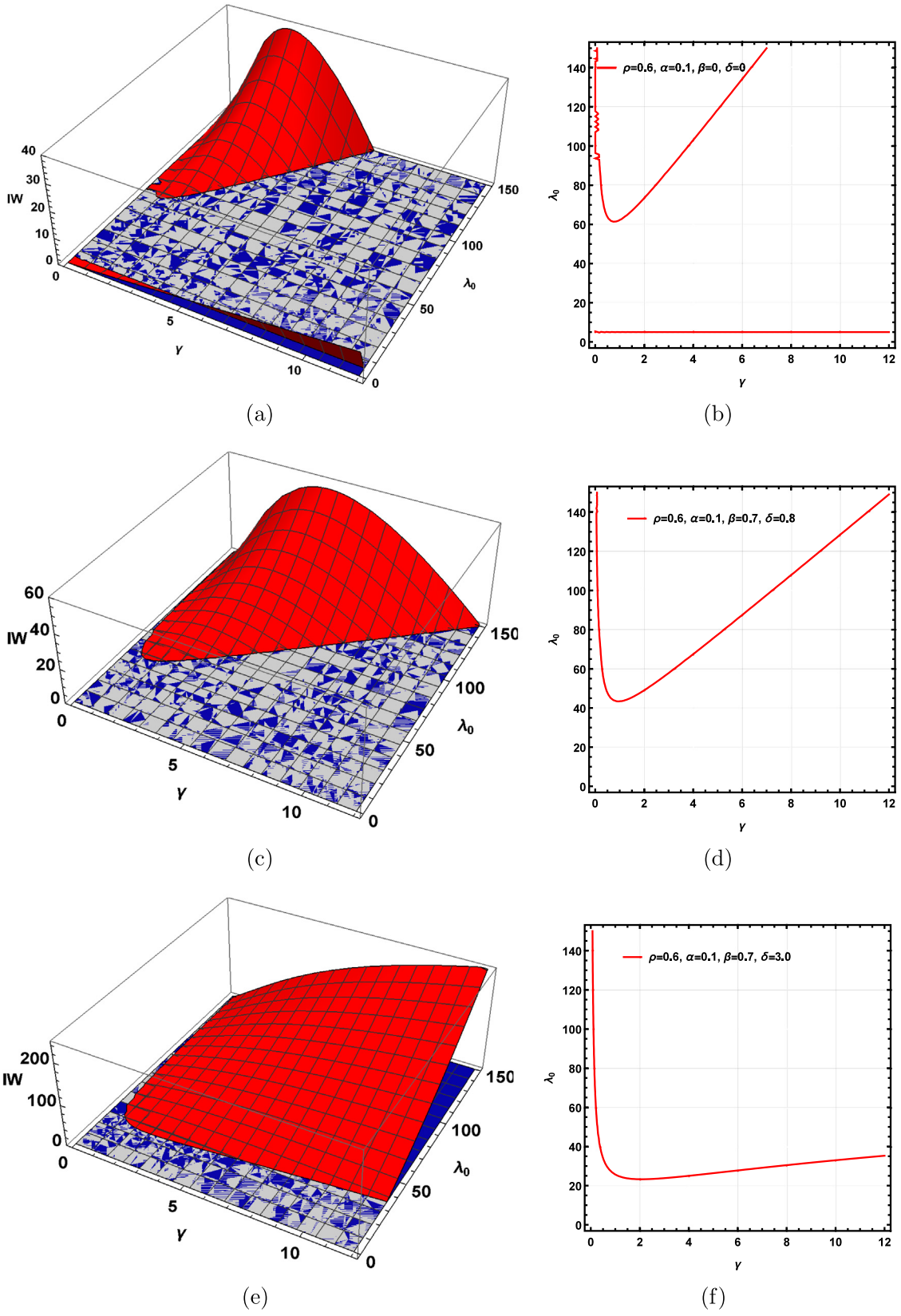

Fig. 4. Illustration of the changes incurred in the size of the instability window in the $\gamma - \lambda_0$ (where $\lambda_0 = \lambda(0)$) plane for different choices of $\beta \in (0, 1 - \alpha/\rho)$ and δ. In each of the Figs. 4(b)–4(f), $\alpha = 0.1$ and $\rho = 0.6$, fixed. The region where $IW < 0$ (grayish blue region) corresponds to the region where $0 < \xi < 1$, the linear stability region, while the region where $IW > 0$ corresponds to the region where $\xi > 1$, the oscillatory region. The emergence of a Hopf bifurcation occurs when $IW = 0$ which corresponds to $\xi = 1$, indicated by the 2-D plots.

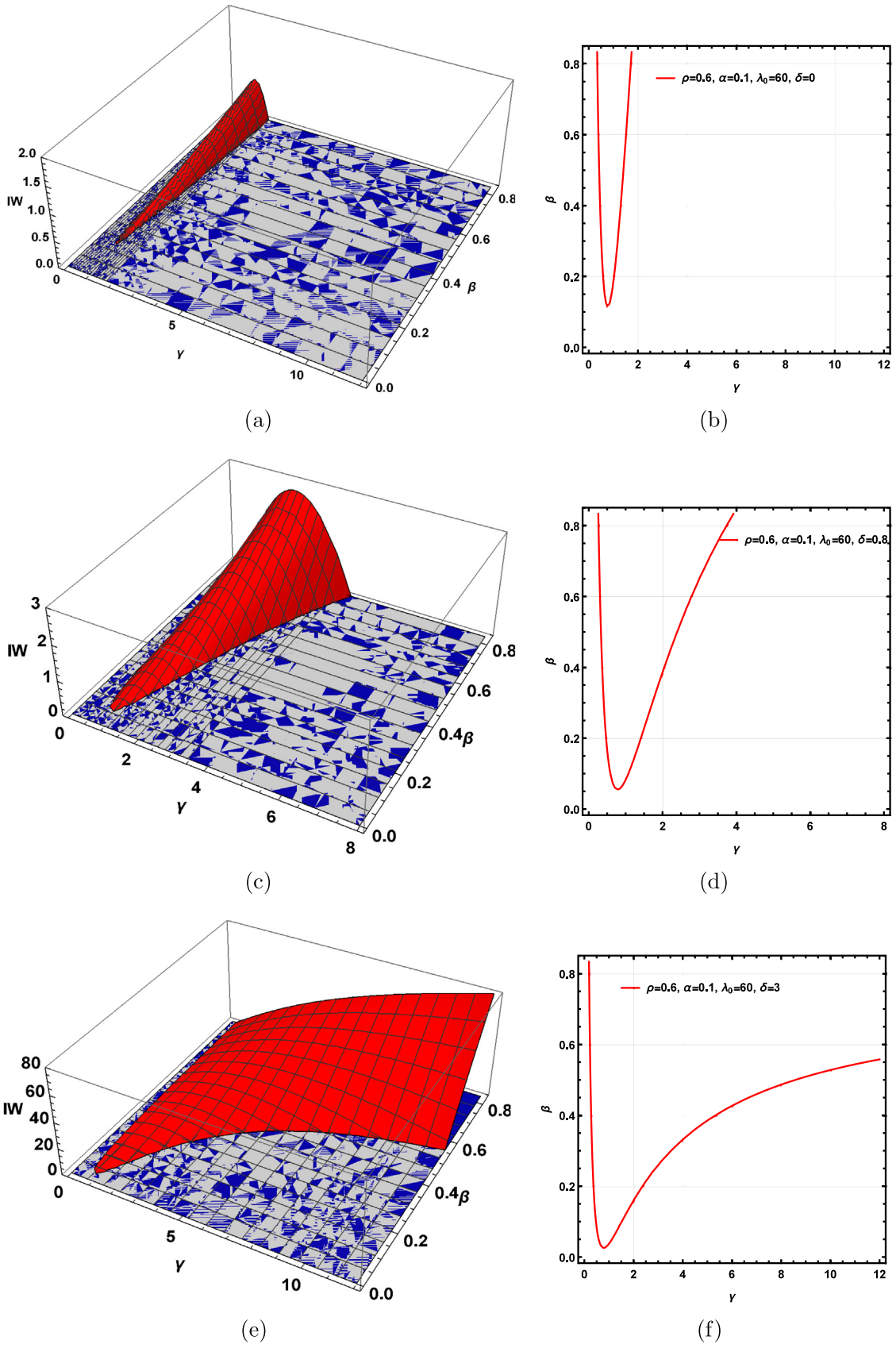

Fig. 5. Illustration of the changes incurred in the size of the instability window in the $\gamma - \beta$ plane as, $\beta \in (0, 1 - \alpha/\rho)$, for different choices of δ and $\lambda(0) = \lambda_0$. In Figs. 5(b)–5(f), $\alpha = 0.1$ and $\rho = 0.6$, and $\lambda_0 = 60$ fixed. The grayish-blue region where $IW < 0$ $(0 < \xi < 1)$ is where linear stability occurs, while the region where $IW > 0$ (red zone corresponding to $\xi > 1$) is the oscillatory region. The emergence of a Hopf bifurcation occurs when $IW = 0$ equivalent to $\xi = 1$, indicated by the 2-D plots.

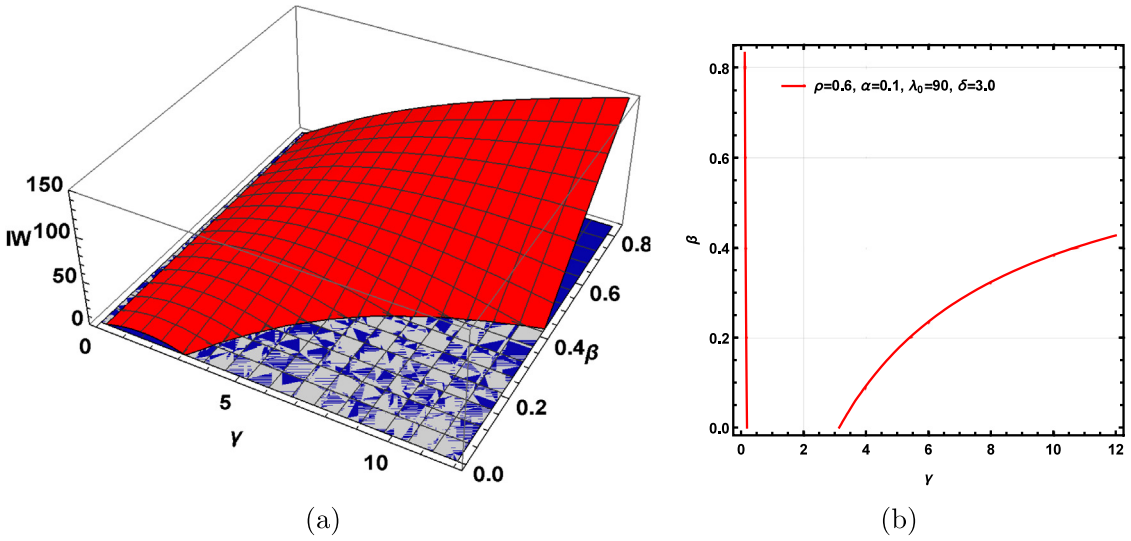

Fig. 6. Illustration of the changes incurred in the size of the instability window in the $\gamma - \beta$ plane as we vary δ, where $\beta \in (0, 1 - \alpha/\rho)$. Here, we increase λ_0 from 60 (the value used in Figs. 5 graphs 5(e)–5(f)) to 90, while maintaining $\alpha = 0.1$, $\rho = 0.6$, and $\delta = 3.0$ fixed. Clearly there are values for γ where we are within the oscillatory regions only.

4.2.6. On the size of the initial amplitude of oscillations at the bifurcation point

We have established, see Appendix B, that the system can be driven to instability via a Hopf bifurcation as the threshold parameter increases from unity. The initial amplitude of the oscillation is given by Eq. (63). At the bifurcation point, we have that the initial growth rate of the exponential growing oscillations is proportional to $\exp(\lambda_r \varepsilon \nu t)$, where we can regard λ_r as a function of β and δ from Eq. (63) we write

$$\lambda_r(\beta, \delta) = \frac{2a_3\omega^2(a_2 - \omega^2)}{4a_3^2\omega^2 + (2a_2 - 4\omega^2)^2}. \tag{49}$$

Thus, as δ and β increase from zero we can compute the initial amplitude of the oscillating solutions which is a positive quantity since $a_2 - \omega^2 = \frac{a_3 a_2 - a_1}{a_3} > 0$ from Eqs. (59) and (60). The size of this growth rate is also different from the base case defined when $\beta = \delta = 0$ and reported in [9], which is $\frac{a_3 a_2}{2(a_2 + a_3^2)}_{|\delta=\beta=0}$ (here a_3 and a_2 are as in Eq. (39)). That is, setting $\beta = \delta = 0$ in Eq. (49) yields $\lambda_r(0,0) = 0 \neq \frac{a_3 a_2}{2(a_2+a_3^2)}_{|\delta=\beta=0}$, since then $\omega^2 = a_2$. There is thus lack of continuity when $\lambda_r(\beta, \delta)$ is regarded as a function of β and δ. Thus in the real sense, we should write

$$\lambda_r(\beta, \delta) = \begin{cases} \frac{2a_3\omega^2(a_2-\omega^2)}{4a_3^2\omega^2+(2a_2-4\omega^2)^2} & \text{if} \quad (\beta, \delta) \neq (0,0) \\ \frac{a_3 a_2}{2(a_2+a_3^2)} & \text{if} \quad (\beta, \delta) = (0,0). \end{cases} \tag{50}$$

This addresses this discontinuity mathematically.

4.2.7. Special case I: Where the waiting time to return to quest is short

In the derivation of Eq. (3), mosquitoes of type W can return to the questing state at rate $c^* = \frac{cH}{H+K}$. Here, c^* is weighted with the dimensionless quantity $\frac{H}{H+K}$, while the actual rate, c, should be interpreted as the reciprocal of the residence time in the W state. Thus, if this residence time is very short, c will be very large and consequently the parameter δ, defined in Eq. (15) will be also be very large. In this case, the W equation given in Eq. (12) will then show a fast reaction sequence, so that the state variable W is essentially in equilibrium with Q and we can evoke the Michaelis–Menten pseudo-steady state hypothesis, [54], and approximate W with Q for all times so that the system with waiting class can be approximated by the system

$$\begin{aligned} \frac{dB}{dt} &= \alpha R\lambda(R) + \alpha R - \rho B, \\ \frac{dQ}{dt} &= \gamma(B - (1-\beta)Q), \\ \frac{dR}{dt} &= Q - R. \end{aligned} \tag{51}$$

$$B(0) = B_0, \quad Q(0) = Q_0, \quad R(0) = R_0.$$

The reduced system (51) has the same steady states as the full system (12), but has the added advantage that we have a reduced dimension in complexity. We provide a detailed study of the stability properties for the non-trivial steady state for the reduced model in Appendix C, where we also demonstrate how to derive the amplitude of the oscillating solutions by approximating the solution on the centre manifold. Fig. 10 shows a phase diagram of the dynamics on the centre manifold illustrating the presence of limit cycles near the origin of the system in the $(u, w)-$phase space where u and w satisfy Eq. (80), a transformed version of the system in Eq. (51).

The dynamical behaviour of the full nonlinear system for the reduced model (51) can be captured by studying and following the progression of the system as the parameters change across different regions of the parameter space as shown in Table 3.

It is informative, in view of studying the properties of the solution in the different regions, to view $\lambda(0)$ as a function of the two parameters β and γ. In this regard, we can fix β and vary γ or fix γ and vary β. The bifurcation diagrams for these two scenarios are shown in Fig. 11.

4.2.8. Special case II: Where the waiting time to return to quest is long

In Eq. (3), mosquitoes of type W can conceivably take a long time to return to the questing state, still at rate $c^* = \frac{cH}{H+K}$, where c is weighted by the dimensionless quantity $\frac{H}{H+K}$. Since the actual rate, c, can be interpreted as the reciprocal of the residence time in the W state, a long waiting time implies that $c \approx 0$ and thus $c^* \approx 0$. Therefore $\beta \approx 0$ with δ, defined in Eq. (15), now satisfying $\delta \approx \frac{\mu_y}{a+\mu_W}$. In this case, the W equation given in Eq. (12) decouples, satisfying a linear equation which is dependent on the solution for Q and system (12) can be approximated by the system

$$\begin{aligned} \frac{dB}{dt} &= \alpha R\lambda(R) + \alpha R - \rho B, \\ \frac{dQ}{dt} &= \gamma(B - Q), \\ \frac{dR}{dt} &= Q - R, \\ \frac{dW}{dt} &= \delta(Q - W) = \delta Q - \delta W. \end{aligned} \tag{52}$$

$$B(0) = B_0, \quad Q(0) = Q_0, \quad R(0) = R_0.$$

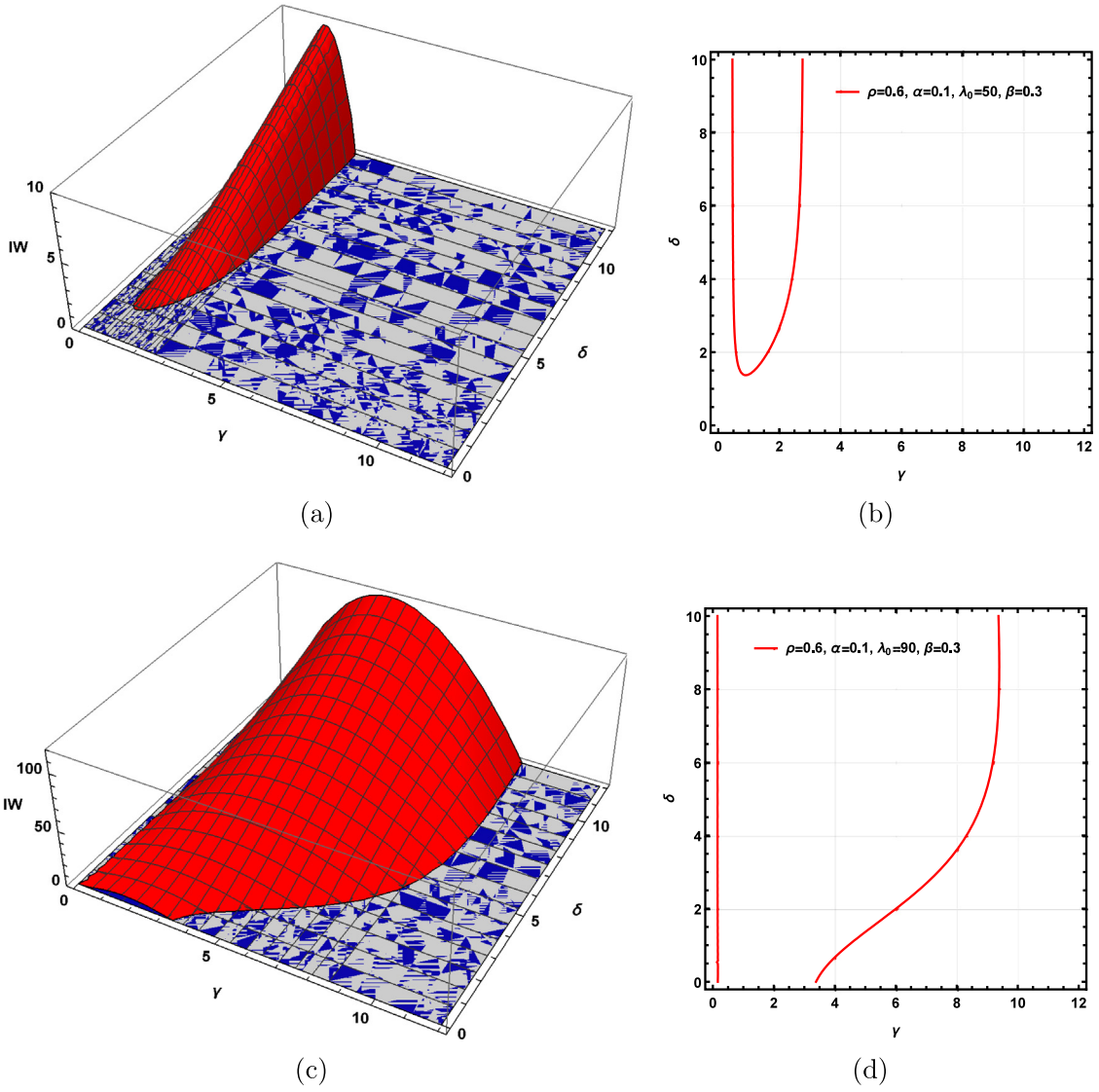

Fig. 7. Illustration of the changes incurred in the size of the instability window in the $\gamma - \delta$ plane, for $\beta = 0.3$ and for $\lambda(0) = \lambda_0 \in \{50, 90\}$ fixed, with $\alpha = 0.1$ and $\rho = 0.6$, fixed. Again, the region where $IW < 0$ (grayish blue region) corresponds to the region where $0 < \xi < 1$, the linear stability region, while the region where $IW > 0$ corresponds to the region where $\xi > 1$, the oscillatory region. The emergence of a Hopf bifurcation occurs when $IW = 0$ which corresponds to $\xi = 1$, indicated by the 2-D plots.

The reduced system (52) is thus mainly driven by the first three equations, which is the model without waiting class mosquitoes studied in detail in [9]. Once Q is known, then the solution for the waiting class mosquitoes is just the solution to the linear differential equation $\frac{dW}{dt} + \delta W = \delta Q$. Thus, the dynamics of the said system is already known.

4.2.9. Relating to the original parameters of the system

We note from the explorations given above that though the upgraded system has richer dynamics and predicts greater possibilities for resilience by the mosquitoes, the qualitative results are the same as before: There exists a threshold parameter that determines the existence of non-zero steady state solutions, and whose size can be used as an indicator for the existence of a Hopf bifurcation in model equations. The main difference here being that while in the simplified model, one could uniquely regard an increase in the threshold parameter as an increase in the birth rate constant, $\lambda(0)$, we now have two new parameters β and δ whose sizes can also influence the size of the threshold parameter. We must recall that $\beta = q\left(\frac{c^*}{c^*+\mu}\right)\left(\frac{\tau^*}{\tau^*+\mu}\right)$, so it is easy to see that β is an increasing function of c^*. Thus $\mathcal{N}$ is an increasing function of c^* since $\mathcal{R}_m$, ρ and α are independent of c^*. This tells us that the non-stabilising effect comes from mosquitoes in the waiting class returning to the human habitats to quest for a blood meal. Thus even when $\mathcal{R}_m < 1$, it is possible for mosquitoes in the waiting class to drive the value of $\mathcal{N}$ above one. In addition to the control measures seen earlier, the model with multiple feeding attempts suggests that receptacles that can serve as temporal waiting sites in our environment should be destroyed. This will reduce c^* as possible waiting sites will be at a considerable distance from the human habitats.

5. Discussion and conclusions

Many infectious diseases of humans, including malaria, yellow fever, Zika and more, are transmitted from human to human by female mosquitoes, which from time to time visit humans at human habitat sites to quest for blood needed for the maturation of their eggs. When a mosquito searches and bites a human for blood, where there is infection either in the mosquito or the human, the infection can be transferred from the one party to the other. It is therefore of paramount interest for human health systems, for people residing in mosquito infested and malarious, yellow fever, dengue fever and zika zones, that we understand the dynamics of populations of the mosquito.

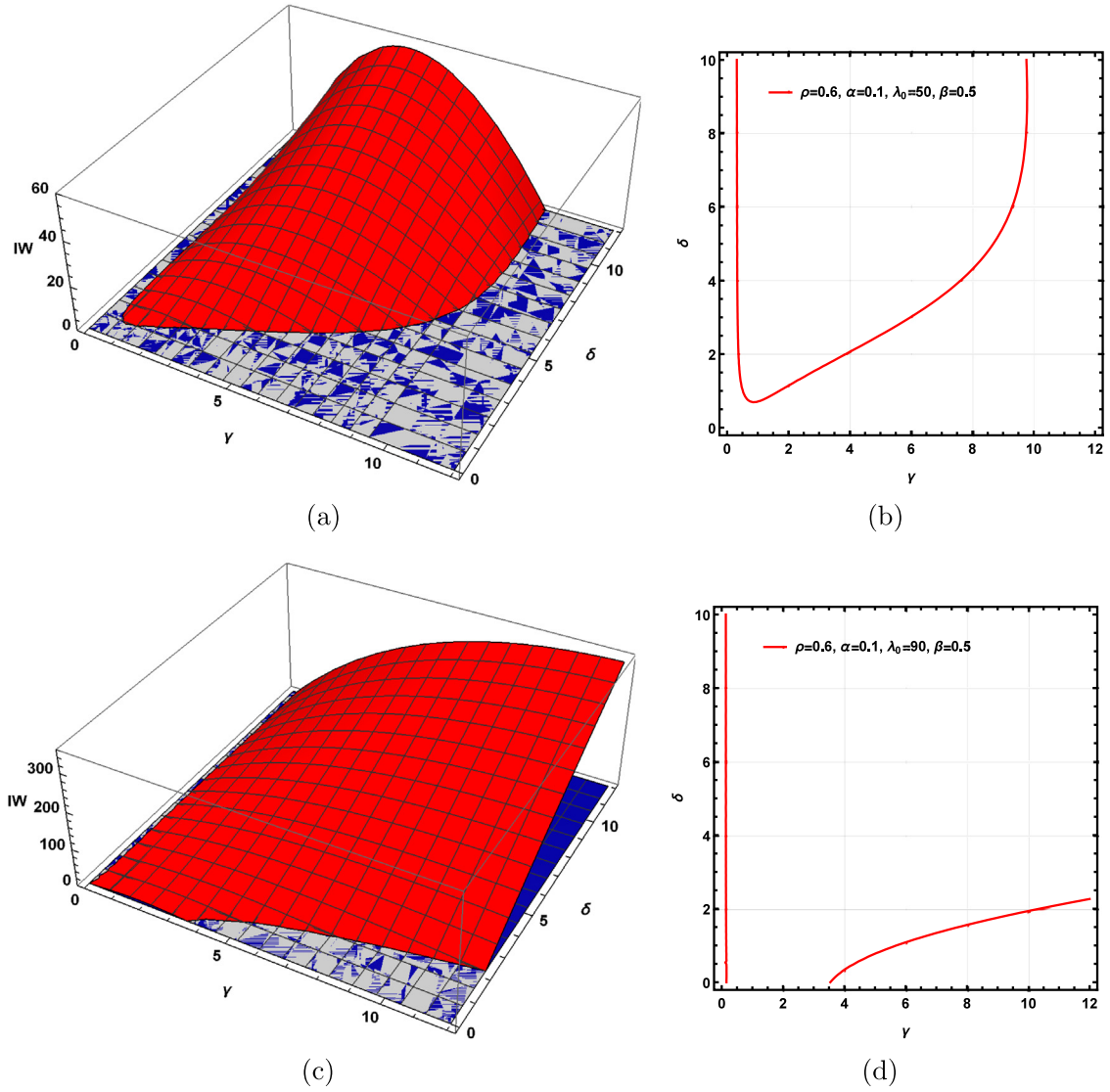

Fig. 8. Illustration of the changes incurred in the size of the instability window in the $\gamma - \delta$ plane, for $\beta = 0.5$ and for $\lambda_0 \in \{50, 90\}$ fixed, with $\alpha = 0.1$ and $\rho = 0.6$, fixed. Again, the region where $IW < 0$ (grayish blue region) corresponds to the region where $0 < \xi < 1$, the linear stability region, while the region where $IW > 0$ corresponds to the region where $\xi > 1$, the oscillatory region. The emergence of a Hopf bifurcation occurs when $IW = 0$ which corresponds to $\xi = 1$, indicated by the 2-D plots.

A framework for studying the dynamics of mosquito populations, that captures the blood feeding habit of the mosquitoes, was developed in [9]. In that first paper, it was assumed that any mosquito that attempts to feed on a human and did not succeed in that first attempt also died in the process. This assumption, which was then used to measure human's success in using insecticide impregnated bed nets [55], is unrealistic because not all mosquitoes that engage to feed on a human and fail do die in the process. It is desirable, therefore, to assume that a mosquito that attempted to feed and did not succeed (perhaps because it was disturbed during the feeding process), but survived the encounter, would be driven to attempt to feed again by its reproductive need. There may be several reasons, including the fact that the mosquito may be infected with a pathogen, why a mosquito would attempt to feed multiple times during one questing episode. In one study, it was discovered that when the duration of contact with a host is limited, infected mosquitoes make more attempts at probing before being successful at taking a blood meal, [56]. There is therefore a possibility that transmission of infection from mosquito to humans maybe continually enhanced by the infection causing the mosquito to probe more for blood meals. In this paper we addressed the problem of multiple feeding by mosquitoes by extending the model originally studied in [9] to include this multiple feeding aspect.

The extension we made on the model was to include a waiting class whereto surviving mosquitoes that failed to take a blood meal after interacting with humans could go into, and from where they can make the next attempt to blood feed on the humans. The institution of the waiting class came along with some important changes in the dynamics. It now becomes important to discuss issues relating to the length of time the mosquitoes would stay in the waiting class state before returning to feed. In a more general setting it will also be important to discuss on whether or not the mosquito in the waiting class would return to the same vertebrate host or choose another. The inclusion of the waiting class also brought to the fore the question of defining what we mean by a "transition" and what we interpret as "new recruits" in relation to the mosquitoes in the system.

Examination of different transition patterns gave rise to two threshold parameters that could be used to study the dynamics of populations of mosquitoes. We gave meaning to different transition patterns by regarding the mosquito's reproductive pathway or gonotrophic cycle; the cycle comprising the steps of leaving the breeding site to the

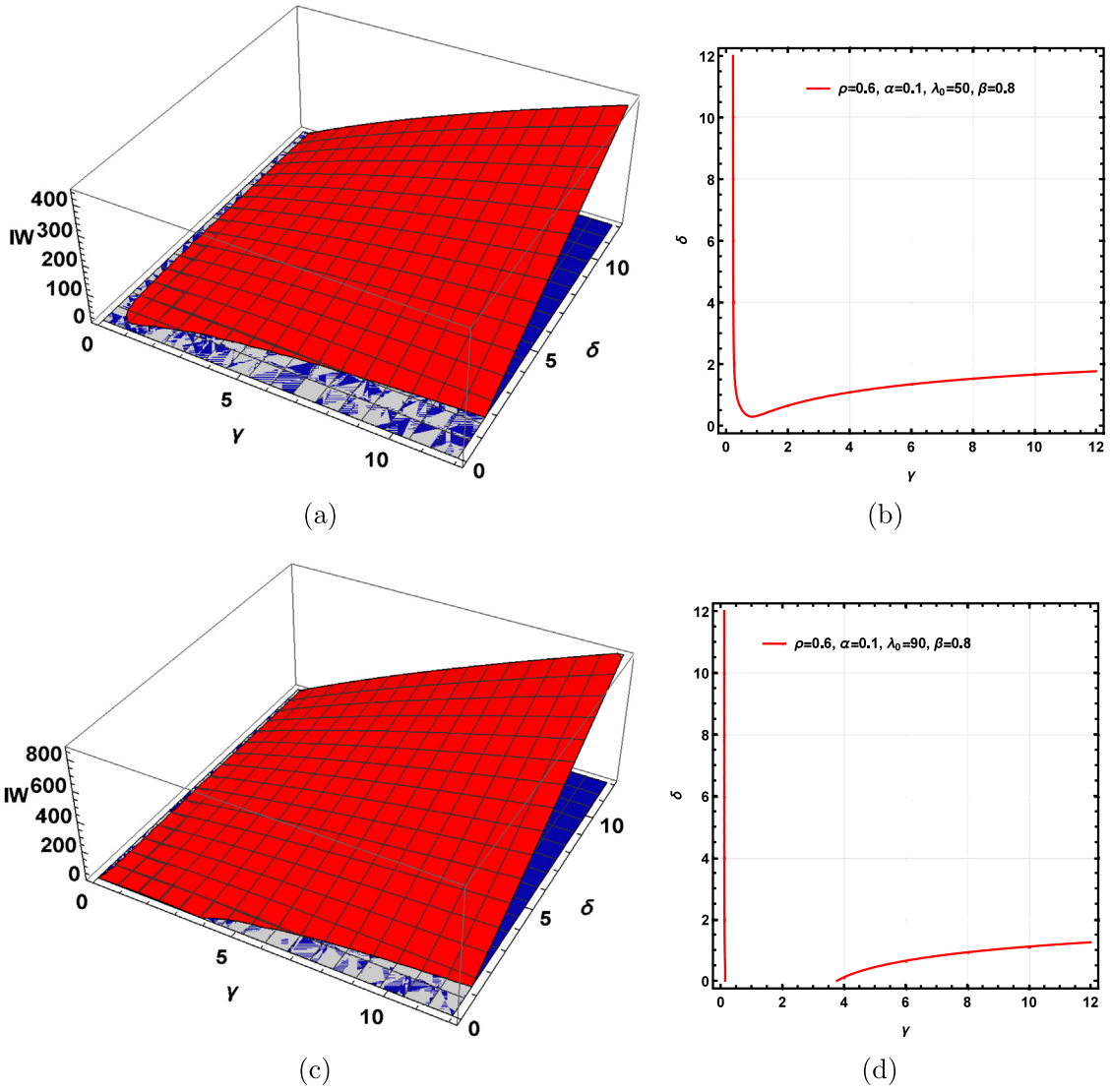

Fig. 9. Illustration of the changes incurred in the size of the instability window in the $\gamma - \delta$ plane, for $\beta = 0.8$ and for $\lambda_0 \in \{50, 90\}$ fixed, with $\alpha = 0.1$ and $\rho = 0.6$, fixed. Again, the region where $IW < 0$ (grayish blue region) corresponds to the region where $0 < \xi < 1$, the linear stability region, while the region where $IW > 0$ corresponds to the region where $\xi > 1$, the oscillatory region. The emergence of a Hopf bifurcation occurs when $IW = 0$ which corresponds to $\xi = 1$, indicated by the 2-D plots.

Table 3
The parameter space is delimited by parameter groupings whose size determines the behaviour of the system changing the qualitative properties of the solutions of the system. The first bifurcation point is where $\lambda(0) = \lambda_m(\beta) = \frac{\rho(1-\beta)-\alpha}{\alpha}$. The second bifurcation point occurs ate $\lambda(0) = \lambda_c(\beta,\gamma) = \lambda_m(\beta) + \frac{a_2(\beta,\gamma)a_1(\beta,\gamma)}{a\gamma}$. The interval $0 \le \lambda(0) < \lambda_m(\beta)$ corresponds to the interval $0 \le \mathcal{N} < 1$ in terms of the threshold parameter $\mathcal{N}$. The second interval $\lambda_m(\beta) < \lambda(0) < \lambda_c(\beta,\gamma)$ corresponds to the interval $1 \le \mathcal{N} < N_c(\beta,\gamma)$.

Region	Description of the parameters	Properties of the system
Reg I	$0 \le \lambda(0) \le \lambda_m(\beta)$	The system has a uniquely determined steady state: the trivial steady state, that is globally and asymptotically stable for all parameter regimes
Reg II	$\lambda_m(\beta) < \lambda(0) < \lambda_c(\beta,\gamma)$	**(i)** The trivial steady state loses stability but still coexists with a non trivial steady state which become existent as $\lambda(0)$ becomes larger than $\lambda_m(\beta)$ **(ii)** The newly created non trivial steady state is linearly stable for these value of the parameters
Reg III	$\lambda = \lambda_c(\beta,\gamma)$	**(i)** The trivial steady state still coexists with a non trivial steady state. **(ii)** The non trivial steady state's stability properties changes from a stable nodes to a centre. This is a Hopf bifurcation point
Reg IV	$\lambda > \lambda_c(\beta,\gamma)$	Growing oscillations with positive real parts are observed in this region. The nonlinearity in the system then bounds the exponential growth leading to bounded and stable limit cycle solutions

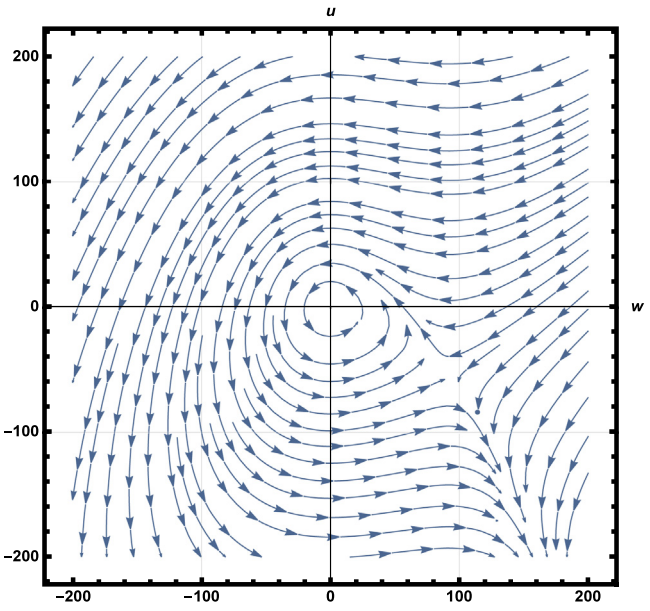

Fig. 10. Figure showing the dynamic of the flow in closed cycles near the origin on the centre manifold for the reduced system (51) as approximated by system (80). The dynamics here are generated using the logistic function $\lambda(u) = \lambda(0)(1-u)$ alongside the parameters $\gamma = 2$, $\rho = 0.8$, $\alpha = \frac{3}{4}\rho$, $\beta = \frac{\rho-\alpha}{2\rho}$, $\lambda(0) = \frac{(1-\beta)\rho-\alpha}{\alpha} + \frac{a_2 a_1}{a\gamma}$, where the parameter groupings a_2 and a_1 are as described in the text in Appendix C.

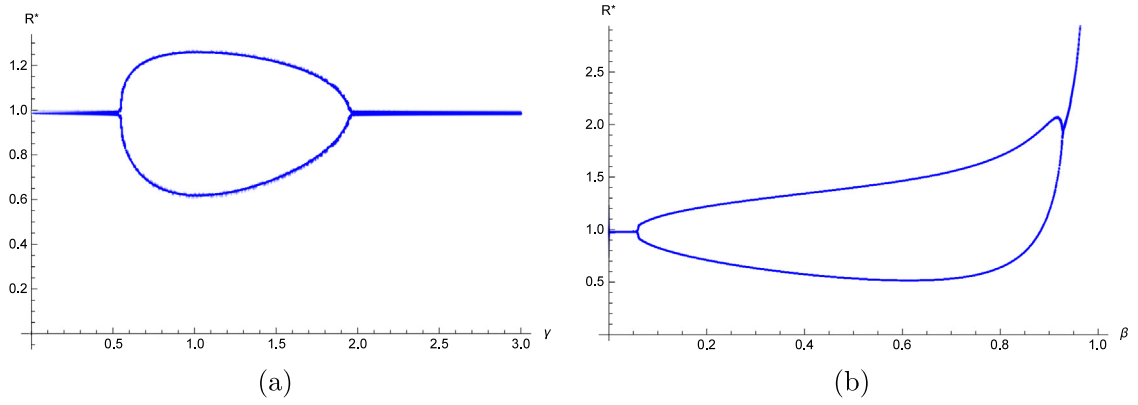

Fig. 11. Illustration of the bifurcation diagram for the full nonlinear system for the model (51) with fast W dynamics. The parameter values are the same as those in Fig. 10 except that in Fig. 11(b), for a fixed value of β and also $\lambda(0)$, γ was allowed to vary and the final amplitude of the solution for R is collected for each value of γ. In Fig. 11(a), all parameters are fixed and β is allowed to vary over its domain. In both cases, we clearly see how the amplitude of the solutions goes from fixed amplitude to varying amplitude and back to fixed amplitude as was predicted.

human habitat, harvesting a blood meal, resting and returning to the breeding site to lay eggs, as the natural path. It was then possible to consider two ways of entering this path: One way as newly emerging adult mosquitoes from the aquatic stages at the breeding site, and a second way by coming from the waiting compartment back onto the path. These two interpretations gave rise to two plausible threshold parameters that could be used as an indicator for the basic offspring number for the mosquitoes. The discussion as to what constitutes new entries and what constitutes transitions in a compartmental model framework as has been done here, which has been known to influence interpretation of threshold-like parameters in epidemic and ecological models, [49–51], was discussed in the context of mosquito dynamics model for the first time in this paper.

The extended model that we studied in this paper had a realistic non-zero steady-state solution which is stable for certain parameter regimes and can be driven to instability to stable limit cycle solutions via a Hopf bifurcation for other values of the parameters. The oscillatory phenomena, which has been observed and reported before, is an important feature of this class of models as it captures the fact that population densities of mosquitoes fluctuate in time according to the seasons of the year. The leading order term for the period of oscillations was also approximated in terms of the parameters of the model and the effect of the waiting class on the nature of the stability window, the initial period of oscillation and the initial amplitude were fully discussed. The fact that the upgraded model continues to exhibit oscillatory behaviour from the simple assumptions made is an important feature of our modelling framework. It is worth pointing out that the paradigm used in building up this mode brings out the oscillatory dynamics that are known to be present in the dynamics of mosquito populations and consequently the diseases they transmit, without recourse to external seasonal forcing.

By assuming that the waiting time for the mosquitoes to stay in the waiting class is short, we used the pseudo-equilibrium approximation theory to argue that the mosquitoes in the waiting class are in equilibrium with the mosquitoes in the questing class. This enabled us to reduce the dimension of the system by one. A full nonlinear analysis of the reduced model is then possible using the centre manifold theorem [57], and numerical solutions agreed with the analysis conducted.

We compared the results of the model without the waiting class with the results of the model with the waiting class and saw that even though the two models have the same qualitative dynamical properties, the upgraded model has richer dynamics, and also captured the ability of the mosquito to survive as a species. For example, it was possible to establish the existence of a positive non-trivial steady state for the upgraded model in parameter regimes where the model without the waiting class predicted extinction. We interpreted this to mean that allowing the mosquitoes the possibilities for repeated feeding gave the insect a higher chance of succeeding to reproduce.

In terms of control, we are able to report the existence of a threshold parameter, $\mathcal{N}$, which we have identified as the *basic offspring number* or *vectorial reproduction number* with the property that if $0 \leq \mathcal{N} \leq 1$, the trivial steady state of the system is globally asymptotically stable, and if $\mathcal{N} > 1$ mosquito eradication is impossible. The control criterion therefore is to set the parameters of the system such that the basic offspring number stays below unity for a long time. This control parameter is seen to be sensitive to the rate at which mosquitoes lay eggs when the population numbers of egg laying mosquitoes are small as well as on the rate at which the mosquitoes in the waiting class return to the breeding site to feed. In particular, if the flow or exchange rate between waiting class and questing class mosquitoes is very efficient, then the density of breeding site mosquitoes at equilibrium is also small indicating that fewer mosquitoes would complete the gonotrophic cycle eventually leading to control. That is, $\beta \approxeq 1$, $B^* = (1-\beta)R^* \approxeq 0$. This is an important results which we are reporting for the first time: disrupt the flow on the gonotrophic cycle path by providing a bypass state, the waiting class, where the mosquitoes can detour into. The snag here is that there are also values of β at which level the waiting class mosquitoes become a pathway to recovery for the mosquito population when the numbers are small. Creating and sustaining a sizable waiting class can be achieved by a judicious use of repellents and bed nets to curb human–mosquito contact combined with suitable baits to draw the questing mosquitoes into the waiting class.

The results of the current paper are very useful in that they set the stage for the investigation of the impact of multiple probing attempts by mosquitoes on malaria transmission. We have also set the stage for discussing how multiple feeding will impact the population dynamics in a human–mosquito–animal interactive framework. Mating patterns, environmental stochasticity, temperature, precipitation and the availability of breeding sites are all factors that affect the population dynamics of mosquitoes. A clear stratification of the mosquito population into autogenous and anautogenous classes [5], will also affect the human–mosquito–animal interactive framework. These and other aspects of the paper including spatial spread and dispersion of mosquitoes are aspects that are still under consideration.

Code availability

Mathematica code was used and is available on request.

CRediT authorship contribution statement

Bime M. Ghakanyuy: Development and analysis of the paper. **Miranda I. Teboh-Ewungkem:** Development and analysis of the paper. **Kristan A. Schneider:** Reviewed the entire manuscript. **Gideon A. Ngwa:** Development and analysis of the paper.

Declaration of competing interest

The authors declare that they have no known competing financial interests or personal relationships that could have appeared to influence the work reported in this paper.

Acknowledgements

GAN and KAS acknowledge the grants and support of the University of Buea, Cameroon and the Hochschule Mittweida University of Applied Sciences, for a DAAD funded visiting professorship to Germany (Project-ID 57479556). GAN also acknowledges the Cameroonian Ministry of Higher Education through the initiative for the modernisation of research in Cameroon's Higher Education. All authors also acknowledge the sponsorship of the Commission for Developing Countries (CDC) in conjunction with the International Mathematics Union (IMU) through the CDC-ADMP (African Diaspora Mathematicians Program) grant that made it possible for interactive collaborative work during the 2018 and 2019 grant sponsored visits to the University of Buea by MIT-E during which period some of this work was discussed. BMG acknowledges additional support from the CDC-IMU programme for Graduate Assistantship in Developing Countries (GRAID) for the 2019/2020 and 2020/2021 granting seasons. MIT-E also acknowledges the National Science Foundation (NSF) support under the NSF grant 1815912, which enabled her engagement in completing the project.

Funding

IMU/CDC-GRAID Award with program id IMU-GRAID for BMG, DAAD project-ID 57479556 for GAN and KAS, CDC-ADMP award and also NSF award 1815912 for MIT-E.

Appendix A. Model's basic properties

Let $\boldsymbol{x} : \mathbb{R}^+ \longrightarrow \mathbb{R}^4_+$ be the vector valued function such that $\boldsymbol{x}(t) = (B(t), Q(t), W(t), R(t))$, with system (6) written in the form

$$\frac{d\boldsymbol{x}}{dt} = \boldsymbol{f}(\boldsymbol{x}), \quad \boldsymbol{x}(0) = \boldsymbol{x}_0, \tag{53}$$

where $\boldsymbol{f} : \mathbb{R}^4 \longrightarrow \mathbb{R}^4$ is defined as follows: $\boldsymbol{f}(\boldsymbol{x}) = (f_1(\boldsymbol{x}), f_2(\boldsymbol{x}), f_3(\boldsymbol{x}), f_4(\boldsymbol{x}))$, with $f_1(\boldsymbol{x}) = aR\lambda(R)+aR-(b^*+\mu)B$, $f_2(\boldsymbol{x}) = b^*B+c^*W-(\tau^*+\mu)Q$, $f_3(\boldsymbol{x}) = q\tau^*Q-(c^*+\mu)W$ and $f_4(\boldsymbol{x}) = p\tau^*Q-(a+\mu)R$.

Lemma A.1. *The function $\boldsymbol{f}$ in (53) is (locally) Lipschitzian*

Proof. Let $\|\cdot\|_\infty$ be the maximum modulus norm in $\mathbb{R}^4$. Then we easily establish that for $\boldsymbol{x}_1, \boldsymbol{x}_2 \in \mathbb{R}^4_+$, $\|\boldsymbol{f}(\boldsymbol{x}_1) - \boldsymbol{f}(\boldsymbol{x}_2)\|_\infty \leq M\|\boldsymbol{x}_1 - \boldsymbol{x}_2\|_\infty$, where $M = \max\{M_1, M_2, M_3, M_4\}$ with $M_k = \max\left\{\left|\frac{\partial f_k}{\partial x_j}\right|, x_j \in \{R, B, Q, W\}\right\}$. $M < \infty$ since $R\lambda(R)$ is differentiable and bounded whenever the initial condition $R_0 \in [0, L)$, where L is the corresponding carrying capacity of the system. For the logistic model we can at best surmise that $R\lambda(R)$ is locally bounded, within the set $[0, L)$, from continuity arguments. □

Theorem A.1 (*Existence and Uniqueness of Solutions*)**.** *The differential Eq. (53) has a unique solution.*

Proof. Since $\boldsymbol{f}$ is Lipschitz continuous with respect to $\boldsymbol{x}$ and continuous with continuous t, we conclude by the Picard's existence and uniqueness theorem that system (53) has a unique solution which is defined in some neighbourhood of the initial condition $(t_0, \boldsymbol{x}(t_0)) = (t_0, \boldsymbol{x}_0)$. □

Theorem A.2 (*Positivity*)**.** *Let $\mathbb{G} = \{(B, Q, W, R) \in \mathbb{R}^4 : B, Q, W, R \in \mathbb{R}^+\}$. If the initial conditions of system (53) lies in $\mathbb{G}$, then the unique solutions characterised by Theorem A.1 lie in $\mathbb{G}$, whenever it exists.*

Proof. Assume for a contradiction that there exists a first time t_1 such that $X(t_1) = 0$, $\frac{dX(t_1)}{dt} < 0$ for $0 < t \leq t_1$, $\mathbf{X}(t) \in \mathbb{G}\backslash\{0\}$ where $X \in \{B, Q, W, R\}$. Now, when $X = B$,

$$\frac{dB(t_1)}{dt} = aR\lambda(R) + aR > 0.$$

For $X = Q, W$ and R, we have respectively that

$$\frac{dQ(t_1)}{dt} = b^*B + c^*W > 0, \quad \frac{dW(t_1)}{dt} = q\tau^*Q > 0, \quad \frac{dR(t_1)}{dt} = p\tau^*Q > 0$$

which contradicts the assumption $\frac{dX(t_1)}{dt} < 0$. Thus no such t_1 exists. □

Theorem A.3 (*Boundedness*). *The unique solution characterised by Theorem A.1 is bounded.*

Proof. From the nature of $\lambda(R)$, $R\lambda(R)$ is bounded above for all $R \geq 0$ or on a restricted domain $(0, L)$.[6] Suppose this bound is $\lambda_m = R_m\lambda(R_m)$ which is obtained by finding R_m such that $\lambda(R_m) + R_m\lambda'(R_m) = 0$. Consider system (6) and let $T_m(t) = B(t) + Q(t) + W(t) + R(t)$ with $T_m(0) = B(0) + Q(0) + W(0) + R(0)$. Then T_m satisfies the equation

$$\frac{dT_m}{dt} = aR\lambda(R) - (1-p)(1-\theta)\tau^*Q - \mu_B B - \mu_Q Q - \mu_W W - \mu_R R, \quad (54)$$

since $q = \theta(1-p)$. Let $\mu = \max\{\mu_B, \mu_Q, \mu_W, \mu_R\}$. Then from (54) we have that

$$\frac{dT_m}{dt} \leq a\lambda_m - \mu T_m \Rightarrow T_m(t) \leq T_m(0)e^{-\mu t} + \frac{a\lambda_m}{\mu} - \frac{a\lambda_m}{\mu}e^{-\mu t}. \quad (55)$$

From (55), we see that the size of T_m is bounded above by a quantity that converges to $\frac{a\lambda_m}{\mu}$ as $t \to \infty$. In particular, if $T_m(0) \leq \frac{a\lambda_m}{\mu}$, then $T_m(t)$ is bounded from above by $\frac{a\lambda_m}{\mu}$. If $T_m(0) > \frac{a\lambda_m}{\mu}$, we have from (55) that

$$\limsup_{t\to\infty} T_m = \frac{a\lambda_m}{\mu}.$$

□

Appendix B. Stability of the non-trivial steady state and Hopf bifurcation

In this section we show that there exists region in parameter space for which the non-trivial steady state is asymptotically stable and points where the system loses stability via a Hopf bifurcation to oscillatory solutions.

Theorem B.1. *Let $\mathcal{N} > 1$ and let R^* be the value of R for which the non-trivial steady state solution prescribed by Theorem 3.1, which is guaranteed to exist only for those parameters for which $\mathcal{N} > 1$, is defined. Let $a_i, i = 1, 2, 3$ be the coefficients in the characteristic polynomial (24). Let us define*

$$\xi = \frac{-a_3^2\gamma\alpha\delta R^*\lambda'(R^*)}{a_1a_2a_3 - a_1^2}. \quad (56)$$

Then, the non-zero steady state solution of the entire system, which corresponds to $R^* > 0$, is linearly stable to small perturbations whenever $\xi < 1$.

Proof. The requirement that $\mathcal{N} > 1$ for the nontrivial steady state to exists follows from Remark 3.2, here, as before, we use $\mathcal{N}$ in place of any one of the two threshold parameters shown in Eqs. (20) and (21). At the non-zero steady state, the coefficients a_1 and a_0 in the characteristic polynomial (24) become

$$a_1 = \gamma\rho\beta + \rho\delta + \gamma\delta(1+\rho)(1-\beta) - \gamma\alpha R^*\lambda'(R^*);$$
$$a_0 = -\gamma\alpha\delta R^*\lambda'(R^*).$$

For linear stability, we note that since λ is monotone decreasing and $1 > \beta$, $a_i > 0$, $i = 0, 1, 2, 3$ we only require, from the Routh–Hurwitz conditions, that

$$a_1a_2a_3 - a_1^2 - a_3^2a_0 > 0 \iff a_1a_2a_3 - a_1^2 + a_3^2\gamma\alpha\delta R^*\lambda'(R^*) > 0 \iff \xi < 1. \quad \square$$

[6] The restricted case applies to the logistic model for example.

Since the coefficients of (24) are all positive whenever $\mathcal{N} > 1$, there are no sign changes in the sequence of coefficients $\{1, a_3, a_2, a_1, a_0\}$ indicating absence of a positive real roots of the polynomial. Letting $\zeta = -\omega$, the Characteristic polynomial becomes

$$\Rightarrow P_4(\omega) = \omega^4 - a_3\omega^3 + a_2\omega^2 - a_1\omega - \gamma\alpha\delta R^*\lambda'(R^*)$$

which has four sign changes in its sequence of coefficients indicating the presence of 4,2 or 0 negative real roots. The complex roots, whenever they exist, occur in conjugate pairs. Thus we can either have: a conjugate pair of complex roots and two negative real roots, two pairs of a conjugate pair of complex roots with no real solution, or four negative real solutions. This suggest that R^* can lose its stability only to oscillatory instabilities as the parameter ξ defined in (56) grows above unity. We now show that there is a choice for the parameter of the system and ξ which for Eq. (24), admits a pair of purely imaginary roots (with the remaining two having negative real parts) and use this fact to deduce that our system admits a Hopf bifurcation.

Lemma B.1. *Let ξ be as defined in (56), which defines a value for a_0 in terms of a_1, a_3 and a_2. At $\xi = \xi_c = 1$, the characteristic polynomial (24) has a pair of distinct roots $\pm i\omega$ on the imaginary axis and the other two roots in the left hand plane.*

Proof. We can rewrite Eq. (24) in terms of ξ as

$$P_4(\zeta) = \zeta^4 + a_3\zeta^3 + a_2\zeta^2 + a_1\zeta + \xi\frac{(a_1a_2a_3 - a_1^2)}{a_3^2} \quad (57)$$

At $\xi = \xi_c = 1$, Eq. (57) factors well into two parts

$$P_4(\zeta) = \zeta^4 + a_3\zeta^3 + a_2\zeta^2 + a_1\zeta + \frac{(a_1a_2a_3 - a_1^2)}{a_3^2}$$
$$= \left(\zeta^2 + \frac{a_1}{a_3}\right)\left(\zeta^2 + a_3\zeta + a_2 - \frac{a_1}{a_3}\right). \quad (58)$$

Since a_1 and a_3 are both positive, the purely imaginary root can be read off from the last expression in (58). The other two roots will have negative real parts whenever $a_0 = \frac{(a_1a_2a_3 - a_1^2)}{a_3^2} > 0$ which translates to the condition $a_3a_2 - a_1 > 0$ so that at the point $\xi = \xi_c = 1$. Using the quadratic formula we then compute all the roots of the polynomial at the critical point to be

$$\zeta_\pm = \pm i\omega = \pm i\sqrt{\frac{a_1}{a_3}} \quad \Rightarrow a_1 = a_3\omega^2 \quad \text{and} \quad \zeta_{1,2} = \frac{-a_3 \pm \sqrt{a_3^2 - \frac{4(a_2a_3 - a_1)}{a_3}}}{2}. \quad (59)$$

Since $a_2a_3 - a_1 > 0$, these two roots are real and negative if $a_3^2 > \frac{4(a_2a_3 - a_1)}{a_3}$ and are complex with negative real part when $a_3^2 < \frac{4(a_2a_3 - a_1)}{a_3}$. □

Remark B.1. The result of Theorem B.1 assures us that the eigenvalues of the linearised system can have negative real parts if $0 \leq \xi < 1$, and that there may be solutions with positive real part if $\xi > 1$, so that a bifurcation can occur in parameter space at the point where $\xi = \frac{a_3^2a_0}{a_1a_3a_2 - a_1^2}$, defined by Eq. (56), is such that $\xi = 1$. The condition $\xi = 1$ translates into two important relations in terms of the coefficients of the characteristic polynomial (24), namely;

$$(i)\ a_3a_2 - a_1 > 0, \quad (ii)\ a_0 = \frac{a_1}{a_3}\left(a_2 - \frac{a_1}{a_3}\right). \quad (60)$$

The next result, which requires notions of subspaces, guarantees the existence of a centre manifold to system (6). We recall the following:

Definition B.1. Let $\sigma(Df(x^*))$ be the set of eigenvalues of the operator D on the vector field $f(x^*)$ and let $\sigma_s = \{\lambda \in \sigma(Df(x^*)) : Re\lambda < 0\}$. Then, E^s, the generalised eigenspace of σ_s, is called a stable subspace of

the vector field $\boldsymbol{f}$. Similarly, if we let $\sigma_c = \{\lambda \in \sigma(D\boldsymbol{f}(\boldsymbol{x}^*)) : Re\lambda = 0\}$, then E^c, the generalised eigenspace of σ_c, is called the centre subspace of the vector field $\boldsymbol{f}$.

Theorem B.2. *Let ξ be as defined in Eq. (56). At $\xi = \xi_c = 1$, E^c and E^s are nonempty and there exists a two dimensional centre manifold, W^c, tangent to the centre subspace E^c and a two dimensional stable manifold, W^s tangent to the stable subspace E^s.*

Proof. We show that $E^c, E^s \neq \emptyset$ by showing that σ_c and σ_s are not empty. At $\xi = \xi_c = 1$, we clearly see from Lemma B.1 that $\sigma_c \neq \emptyset$. The remaining eigenvalues are given by $\xi_{1,2} = \frac{-a_3 \pm \sqrt{a_3^2 - \frac{4(a_2a_3-a_1)}{a_3}}}{2}$, as in Eq. (59). In particular, the following are possible:

1. $a_3^2 - \frac{4(a_2a_3-a_1)}{a_3} \geq 0$, in which case, there are two negative real roots, since $a_3 \geq \sqrt{a_3^2 - \frac{4(a_2a_3-a_1)}{a_3}}$.
2. $a_3^2 - \frac{4(a_2a_3-a_1)}{a_3} < 0$, in which case, there are a pair of complex roots with negative real parts.

In either case, σ_s is also not empty. The existence of two manifolds: W^c and W^s tangent respectively to E^c and E^s follows from the centre manifold theorem [53]. □

Theorem B.3. *Let ξ be defined as in Eq. (56). If the zeros of Eq. (57) depend analytically on ξ, then as ξ increases through $\xi_c = 1$, the non-zero steady state as given in Eq. (16) bifurcates to periodic solutions whose initial period and amplitude can be determine as a function of the perturbation of ξ from $\xi_c = 1$.*

Proof. We use the result of a theorem[7] of Brillinger [58] to deduce that ζ is an analytic function of ξ and write $\zeta = \zeta(\xi)$. Then, denote the pair of purely imaginary roots guaranteed by Lemma B.1 by $\zeta(\xi_c) = \pm i\omega$. Let $0 < \varepsilon \ll 1$ and $\xi = \xi_c + \varepsilon\nu$. So, we choose a positive $\varepsilon \ll 1$ such that $\varepsilon^2 \approx 0$ and $\nu = \pm 1$. Notice that this is just a small displacement of ξ from $\xi_c = 1$.

$$\zeta(\xi) = \zeta(\xi_c + \varepsilon\nu) \approx \zeta(\xi_c) + \zeta'(\xi_c)\varepsilon\nu. \tag{61}$$

Substituting (61) in (57), expanding, retaining only linear terms in ε, we have

$$\begin{aligned}&\zeta^4(\xi_c) + 4\zeta^3(\xi_c)\zeta'(\xi_c)\varepsilon\nu + a_3\left[\zeta^3(\xi_c) + 3\zeta^2(\xi_c)\zeta'(\xi_c)\varepsilon\nu\right]\\ &+ a_2\left[\zeta^2(\xi_c) + 2\zeta(\xi_c)\zeta'(\xi_c)\varepsilon\nu\right] + a_1(\zeta(\xi_c) + \zeta'(\xi_c)\varepsilon\nu)\\ &+ (\xi_c + \varepsilon\nu)\frac{(a_1a_2a_3 - a_1^2)}{a_3^2} \approx 0.\end{aligned}$$

But

$$\zeta^4(\xi_c) + a_3\zeta^3(\xi_c) + a_2\zeta^2(\xi_c) + a_1\zeta(\xi_c) + \xi_c\frac{(a_1a_2a_3 - a_1^2)}{a_3^2} = 0$$

since $\zeta(\xi_c)$ is a solution to (57) at ξ_c. Therefore, since the first term of (59), $a_1 = a_3\omega^2$ at the bifurcation, we have that

$$\zeta'(\xi_c) \approx \frac{-\omega^2(a_2 - \omega^2)}{\left[4\zeta^3(\xi_c) + 3a_3\zeta^2(\xi_c) + 2a_2\zeta(\xi_c) + \omega^2a_3\right]}.$$

Here we only examine the contributions from the purely imaginary pair, given by $\zeta(\xi_c) = \pm i\omega$, since the other two roots, given by (59), are real and negative and will contribute only perturbations that decay to zero with time. So the last expression simplifies to

$$\zeta'(\xi_c) = \frac{2a_3\omega^2(a_2 - \omega^2)}{4a_3^2\omega^2 + (2a_2 - 4\omega^2)^2} \pm i\frac{\omega(a_2 - \omega^2)(2a_2 - 4\omega^2)}{4a_3^2\omega^2 + (2a_2 - 4\omega^2)^2}.$$

[7] Theorem [58]: The roots of an nth degree complex polynomial, $P_n(z)$, are analytic functions of the coefficients in the region where $P_n(z) = 0$, while $P_n'(z) \neq 0$ for some z.

We can now write down the constructed linear approximation to ζ as

$$\begin{aligned}\zeta(\xi) &\approx \zeta(\xi_c) + \zeta'(\xi_c)\varepsilon\nu\\ &= \pm i\omega + \left(\frac{2a_3\omega^2(a_2 - \omega^2)}{4a_3^2\omega^2 + (2a_2 - 4\omega^2)^2} \pm i\frac{\omega(a_2 - \omega^2)(2a_2 - 4\omega^2)}{4a_3^2\omega^2 + (2a_2 - 4\omega^2)^2}\right)\varepsilon\nu\end{aligned}$$

Finally, we write the approximation for ζ in the vicinity of the bifurcation point as

$$\begin{aligned}\zeta(\xi) = &\left(\frac{2a_3\omega^2(a_2 - \omega^2)}{4a_3^2\omega^2 + (2a_2 - 4\omega^2)^2}\right)\varepsilon\nu\\ &\pm i\left(\omega + \frac{\omega(a_2 - \omega^2)(2a_2 - 4\omega^2)}{4a_3^2\omega^2 + (2a_2 - 4\omega^2)^2}\varepsilon\nu\right) + O(\varepsilon^2).\end{aligned} \tag{62}$$

Recall that from Eq. (59), $a_1 = a_3\omega^2$ and since $a_1 = a_3a_2$, get $a_2 - \omega^2 > 0$, showing that for $\varepsilon > 0$, when $\nu = 1$, the real part of the perturbation in ζ from ζ_c is positive. That is, as ξ passes through $\xi_c = 1$, the character of the stable stationary equilibrium changes in such a way that oscillatory solutions whose initial amplitude and period of oscillations are respectively approximated by

$$\exp\left(\frac{2a_3\omega^2(a_2 - \omega^2)}{4a_3^2\omega^2 + (2a_2 - 4\omega^2)^2}\varepsilon\nu t\right) \text{ and } \frac{2\pi}{\left(\omega + \frac{\omega(a_2-\omega^2)(2a_2-4\omega^2)}{4a_3^2\omega^2+(2a_2-4\omega^2)^2}\varepsilon\nu\right)} \tag{63}$$

are observed. □

Remark B.2. We have just described conditions for the occurrence of a Hopf bifurcation using the same procedure that was adopted in [9].

Appendix C. Analysing the reduced system: centre manifold approximation

The reduced system for the case of short waiting time is given by Eq. (51). To study the stability of the non-trivial steady state for this reduced system, we shift the nontrivial equilibrium of system (51) to the origin by considering the transformation: $x = B - B^*$, $y = Q - Q^*$ and $z = R - R^*$, where it is known that $Q^* = R^*$, $B^* = (1 - \beta)R^*$, $\alpha R^*\lambda(R^*) + \alpha R^* - \rho B^* = 0$, so that system (51) becomes

$$\begin{aligned}\frac{dx}{dt} &= \alpha(z + R^*)\left[\lambda(z + R^*) + 1\right] - \rho(x + B^*),\\ \frac{dy}{dt} &= \gamma(x - (1 - \beta)y),\\ \frac{dz}{dt} &= y - z.\end{aligned} \tag{64}$$

Consider a Taylor expansion so that $\lambda(z + R^*) = \lambda(R^*) + z\lambda'(R^*) + \frac{1}{2}z^2\lambda''(R^*) + O(z^3)$, and substitute in system (64). We note that when $\lambda(R)$ is the logistic formula as introduced in (1), $\lambda(R^* + z) = \lambda(R^*) + z\lambda'(R^*)$ and we do not need to worry about any higher order approximation terms as all higher order derivatives vanish. When $\lambda(R)$ is a bounded nonlinear function of the other types shown in (1), $\lambda(R^* + z)$ will admit an infinite Taylor expansion. In this case we truncate the expansion as indicated to aim for a manageable quadratic nonlinearity in the reduced system. Next, make use of the fact that (B^*, Q^*, R^*) is an equilibrium point of system (51), then our system (64) reduces to

$$\begin{aligned}\frac{dx}{dt} &= \alpha H(R^*)z - \rho x + \alpha\left(\lambda'(R^*) + \frac{1}{2}R^*\lambda''(R^*)\right)z^2 + O(z^3),\\ \frac{dy}{dt} &= \gamma(x - (1 - \beta)y),\\ \frac{dz}{dt} &= y - z.\end{aligned} \tag{65}$$

We can then rewrite system (65) in the form

$$\frac{d\boldsymbol{x}}{dt} = A\boldsymbol{x} + \boldsymbol{F}(\boldsymbol{x}) \quad \text{where} \quad \boldsymbol{x} = (x, y, z)^T, \tag{66}$$

$$A = \begin{pmatrix} -\rho & 0 & \alpha H(R^*) \\ \gamma & -\gamma(1-\beta) & 0 \\ 0 & 1 & -1 \end{pmatrix} \text{ and } \boldsymbol{F} = \begin{pmatrix} \alpha T(R^*)z^2 + O(z^3) \\ 0 \\ 0 \end{pmatrix}, \tag{67}$$

where

$$T(R^*) = \lambda'(R^*) + \frac{1}{2}R^*\lambda''(R^*) \text{ and } H(R^*) = \lambda(R^*) + R^*\lambda'(R^*) + 1.$$

We can approximate $\boldsymbol{F}$ by ignoring the $O(z^3)$ terms in its definition, while noting that the error for this approximation is in fact zero when λ is the logistic growth function. It is clear that $(0,0,0)$ is now an equilibrium point of Eq. (66). If ζ is an eigenvalue of the matrix A, then ζ satisfies the equation

$$\zeta^3 + a_2\zeta^2 + a_1\zeta + a_0 = 0, \tag{68}$$

where now,

$$a_2 = 1+\rho+\gamma(1-\beta),\ a_1 = \rho+\rho\gamma(1-\beta)+\gamma(1-\beta),\ a_0 = \rho\gamma(1-\beta)-\alpha\gamma H(R^*). \tag{69}$$

At the Hopf bifurcation, $a_0 = a_2a_1$. This corresponds to the point in parameter space where $\alpha H(R^*) = \frac{\rho\gamma(1-\beta)-a_2a_1}{\gamma}$. At this point, the eigenvalues of A, given by the roots of (68), are $\zeta = -a_2$, $\zeta = \pm i\sqrt{a_1}$, with corresponding eigenvectors

$$\boldsymbol{v}_{a_2} = \begin{pmatrix} \frac{\rho\gamma(1-\beta)-a_2a_1}{\gamma(\rho-a_2)} \\ 1-a_2 \\ 1 \end{pmatrix},\ \boldsymbol{v}_{i\sqrt{a_1}} = \begin{pmatrix} \frac{\rho\gamma(1-\beta)-a_2a_1}{\gamma(\rho-i\sqrt{a_1})} \\ 1-i\sqrt{a_1} \\ 1 \end{pmatrix},\ \boldsymbol{v}_{-i\sqrt{a_1}} = \begin{pmatrix} \frac{\rho\gamma(1-\beta)-a_2a_1}{\gamma(\rho+i\sqrt{a_1})} \\ 1+i\sqrt{a_1} \\ 1 \end{pmatrix} \tag{70}$$

The centre manifold theorem [57] guarantees the existence of a centre manifold at the origin in the (x,y,z)-space which corresponds to the steady state $B^* = W^* = R^*$ in the (B,W,R)-space. This centre manifold can be realised when we construct the Jordan decomposition of Eq. (66) as in [53] by applying the transformation $\boldsymbol{x} = M\boldsymbol{u}$, where $\boldsymbol{x} = (x,y,z)^T$ and $\boldsymbol{u} = (v,w,u)^T$, and M is the matrix such that

$$M^{-1}AM = \begin{pmatrix} -a_2 & 0 & 0 \\ 0 & 0 & -\sqrt{a_1} \\ 0 & \sqrt{a_1} & 0 \end{pmatrix}. \tag{71}$$

Here, the matrix M is given by

$$M = \begin{pmatrix} \frac{\rho\gamma(1-\beta)-a_2a_1}{\gamma(\rho-a_2)} & \frac{\rho(\rho\gamma(1-\beta)-a_2a_1)}{\gamma(\rho^2+a_1)} & \frac{\sqrt{a_1}(\rho\gamma(1-\beta)-a_2a_1)}{\gamma(\rho^2+a_1)} \\ 1-a_2 & 1 & -\sqrt{a_1} \\ 1 & 1 & 0 \end{pmatrix}. \tag{72}$$

The first column of M is the eigenvector corresponding to the real and negative eigenvalue $-a_2$, its second column is the real part of the eigenvector corresponding to eigenvalue $-i\sqrt{a_1}$ while its third column its imaginary part. The differential equation $\dot{\boldsymbol{x}} = A\boldsymbol{x} + \boldsymbol{F}(\boldsymbol{x})$ is then transformed to the equivalent system

$$\dot{\boldsymbol{u}} = M^{-1}AM\boldsymbol{u} + M^{-1}\boldsymbol{F}(M\boldsymbol{u}) = \begin{pmatrix} -a_2 & 0 & 0 \\ 0 & 0 & -\sqrt{a_1} \\ 0 & \sqrt{a_1} & 0 \end{pmatrix}\boldsymbol{u} + M^{-1}\boldsymbol{F}(M\boldsymbol{u}). \tag{73}$$

In expanded form, the transformed system (73), takes the form

$$\begin{pmatrix} \dot{v} \\ \dot{w} \\ \dot{u} \end{pmatrix} = \begin{pmatrix} -a_2 & 0 & 0 \\ 0 & 0 & -\sqrt{a_1} \\ 0 & \sqrt{a_1} & 0 \end{pmatrix}\begin{pmatrix} v \\ w \\ u \end{pmatrix} + \begin{pmatrix} B(R^*)(v+w)^2 \\ -B(R^*)(v+w)^2 \\ -\frac{a_2}{\sqrt{a_1}}B(R^*)(v+w)^2 \end{pmatrix} \tag{74}$$

leading to the decomposed system separating the stable manifold defined by the equation

$$\frac{dv}{dt} = -a_2v + B(R^*)(v+w)^2, \tag{75}$$

from the centre manifold defined by the system of equations

$$\frac{d}{dt}\begin{pmatrix} w \\ u \end{pmatrix} = \begin{pmatrix} 0 & -\sqrt{a_1} \\ \sqrt{a_1} & 0 \end{pmatrix}\begin{pmatrix} w \\ u \end{pmatrix} + \begin{pmatrix} -B(R^*)(v+w)^2 \\ -\frac{a_2}{\sqrt{a_1}}B(R^*)(v+w)^2 \end{pmatrix}. \tag{76}$$

From Eq. (75), if $B(R^*) < 0$, then surely this component of the solution decays to zero as t increases so that the nature of the solutions for the full system near the steady state (which now is the origin) can be well approximated by the behaviour of the solutions in the centre manifold defined by Eq. (76). Even if B is non-negative, the form of the nonlinearity suggests that perturbations arising from the stable manifold will decay linearly to zero. We note here that from the definition of the parameters, $a_2 - \rho > 0$ just as $((\beta-1)\gamma\rho + a_2a_1) > 0$, and so the sign of B is determined by that of $T(R^*)$, which is known to be negative for the logistic birth function.

In order to determine the stability of the solution on the centre manifold, use the approximation

$$v = h(w,u) = aw^2 + bwu + cu^2 + O(3), \tag{77}$$

where $O(3)$ is used to indicate terms of the form w^iu^j where $i+j \geq 3$, a, b and c are constants to be determine. This form ensures that $h(\mathbf{0}) = \mathbf{0}$ and $\nabla h(\mathbf{0}) = \mathbf{0}$ which are all conditions for tangency of the centre manifold to the centre subspace at the origin [53,57], namely that

$$\frac{\partial h}{\partial w}\frac{dw}{dt} + \frac{\partial h}{\partial u}\frac{du}{dt} - \frac{dv}{dt} = 0, \tag{78}$$

where $\frac{du}{dt}$, $\frac{dv}{dt}$ and $\frac{dw}{dt}$ are defined by the Eqs. (75) and (76) with v replaced by the indicated approximation. We can retain only second order terms in the approximation of the system on the centre manifold near the origin, so that $(v+w)^2 = (h(u,w)+w)^2 = w^2 + O(3)$ if v is approximated by (77). Now, from the assumed form for v, $\nabla h(w,u) = (2aw+bu, bw+2cu)$. Substituting in (78), expanding and equating powers of u^2, wu and w^2 to zero, so that the approximation is valid to the designated order of accuracy, yields the following equations

$$u^2: \ -\sqrt{a_1}b + a_2c = 0,\ w^2: \ b\sqrt{a_1} + aa_2 - B(R^*) = 0,$$
$$wu: \ -2a\sqrt{a_1} + a_2b + a_2b + 2\sqrt{a_1}c = 0.$$

Solving this system gives us

$$a = \frac{\left(a_2^2+2a_1\right)B(R^*)}{a_2\left(a_2^2+4a_1\right)},\quad b = \frac{2\sqrt{a_1}B(R^*)}{a_2^2+4a_1},\quad c = \frac{2a_1B(R^*)}{a_2\left(a_2^2+4a_1\right)} \tag{79}$$

The centre manifold of (33) can thus be represented in the (w,u) plane by the projection (77) where the coefficients a, b and c are defined in (79). The flow of (33) within the centre manifold is governed by the system

$$\begin{aligned} \frac{d}{dt}\begin{pmatrix} w \\ u \end{pmatrix} &= \begin{pmatrix} 0 & -\sqrt{a_1} \\ \sqrt{a_1} & 0 \end{pmatrix}\begin{pmatrix} w \\ u \end{pmatrix} \\ &\quad + \begin{pmatrix} -B(R^*)(h(w,u)+w)^2 \\ -\frac{a_2}{\sqrt{a_1}}B(R^*)(h(w,u)+w)^2 \end{pmatrix}, \\ &= \begin{pmatrix} 0 & -\sqrt{a_1} \\ \sqrt{a_1} & 0 \end{pmatrix}\begin{pmatrix} w \\ u \end{pmatrix} \\ &\quad + \begin{pmatrix} -B(R^*)w^2 + O(3) \\ -\frac{a_2}{\sqrt{a_1}}B(R^*)w^2 + O(3) \end{pmatrix}. \end{aligned} \tag{80}$$

We can proceed to approximate the system on the centre manifold by neglecting the terms of order three and higher; see, for example, [53, 59]. For some degenerate systems, it may happen that truncating the expansion at order three will lead to a loss of the oscillatory dynamics. However, we do not believe it is the case here. It is evident from the

form of the approximating equations from system (80) that we can have limit cycles in the $(w,u)-$ phase plane near the origin where $(w,u)=(0,0)$ is a steady state for the dynamics on the centre manifold. It is now possible to study the dynamics of the system on the limit cycle be examining closely the behaviour of the two-component system described by system (80). The limit cycle near the origin for the reduced system is illustrated in the streamplot shown in Fig. 10, and the full nonlinear model is simulated and a bifurcation diagram shown in Fig. 11.

References

[1] Center for Disease Control and Prevention, Mosquitoes - Borne Diseases, CDC, Accessed 2021.

[2] Rafael Maciel-de Freitas, Raquel Aguiar, Rafaela V Bruno, Maria Cristina Guimarães, Ricardo Lourenço-de Oliveira, Marcos HF Sorgine, Cláudio J Struchiner, Denise Valle, Scott L O'Neill, Luciano A Moreira, Why do we need alternative tools to control mosquito-borne diseases in latin america? Mem. Inst. Oswaldo Cruz 107 (2012) 828–829.

[3] Miranda I. Teboh-Ewungkem, Gideon A. Ngwa, Mary Y. Fomboh-Nforba, A multistage mosquito-centred mathematical model for malaria dynamics that captures mosquito gonotrophic cycle contributions to its population abundance and malaria transmission, in: Miranda I. Teboh-Ewungkem, Gideon A. Ngwa (Eds.), Infectious Diseases and Our Planet. Mathematics of Planet Earth Series, 7, Springer, 2021.

[4] Michael A. Tolle, Mosquito-borne diseases, Curr. Probl. Pediatr. Adolesc. Health Care 39 (4) (2009) 97–140.

[5] Woodbridge A. Foster, Edward D. Walker, Chapter 15 - mosquitoes (Culicidae), in: Gary R. Mullen, Lance A. Durden (Eds.), Medical and Veterinary Entomology, third ed., Academic Press, 2019, pp. 261–325.

[6] Calistus N. Ngonghala, Miranda I. Teboh-Ewungkem, Gideon A. Ngwa, Observance of period-doubling bifurcation and chaos in an autonomous ODE model for malaria with vector demography, Theor. Ecol. 9 (3) (2016) 337–351.

[7] Calistus N. Ngonghala, Gideon A. Ngwa, Miranda I. Teboh-Ewungkem, Periodic oscillations and backward bifurcation in a model for the dynamics of malaria transmission, Math. Biosci. 240 (1) (2012) 45–62.

[8] Calistus N. Ngonghala, Miranda I. Teboh-Ewungkem, Gideon A. Ngwa, Persistent oscillations and backward bifurcation in a malaria model with varying human and mosquito populations: implications for control, J. Math. Biol. 70 (7) (2015) 1581–1622.

[9] Gideon A. Ngwa, On the population dynamics of the malaria vector, Bull. Math. Biol. 68 (8) (2006) 2161–2189.

[10] Siewe Nourridine, Miranda I. Teboh-Ewungkem, Gideon A. Ngwa, A mathematical model of the population dynamics of disease-transmitting vectors with spatial consideration, J. Biol. Dyn. 5 (4) (2011) 335–365.

[11] L.P. Campbell, C. Luther, D. Moo-Llanes, J.M. Ramsey, R. Danis-Lozano, A. Townsend Peterson, Climate change influences on global distributions of dengue and chikungunya virus vectors, Phil. Trans. R. Soc. B R. Soc. Publ. 370 (1665) (2015) 20140135.

[12] Samantha Roth, Miranda Teboh-Ewungkem, Ming Li, Predicting Suitability of Regions for Zika Outbreaks with Zero-Inflated Models Trained Using Climate Data, Cold Spring Harbor Laboratory, 2019, BioRxiv.

[13] European Center for Disease Prevention and Control, Aedes Aegypti - Factsheet for Experts, ECDC, Accessed 2021.

[14] S.M. Hsu, A.M. Yen, T.H. Chen, The impact of climate on Japanese encephalitis, Epidemiol. Infect. 136 (7) (2008) 980–987.

[15] L.L.M. Shapiro, S.A. Whitehead, M.B. Thomas, Quantifying the effects of temperature on mosquito and parasite traits that determine the transmission potential of human malaria, PloS Biol. 15 (10) (2017) e2003489.

[16] Miranda I. Teboh-Ewungkem, Thomas Yuster, A within-vector mathematical model of Plasmodium falciparum and implications of incomplete fertilization on optimal gametocyte sex ratio, J. Theoret. Biol. 264 (2) (2010) 273–286.

[17] Miranda I Teboh-Ewungkem, Gideon A. Ngwa, COVID-19 in malaria-endemic regions: potential consequences for malaria intervention coverage, morbidity, and mortality, Lancet. Infect. Dis. 21 (1) (2021) 5–6.

[18] D.J. Weiss, A. Bertozzi-Villa, S.F. Rumisha, P. Amratia, R. Arambepola, K.E. Battle, E. Cameron, E. Chestnutt, H.S. Gibson, J. Harris, S. Keddie, J.J. Millar, J. Rozier, T.L. Symons, C. Vargas-Ruiz, S.I. Hay, D.L. Smith, P.L. Alonso, A.M. Noor, S. Bhatt, P.W. Gething, Indirect effects of the COVID-19 pandemic on malaria intervention coverage, morbidity, and mortality in Africa: a geospatial modelling analysis, Lancet. Infect. Dis. 21 (1) (2021) 59–69.

[19] Center for Disease Control and Prevention, Mosquitoes: Mosquito Control - Sterile Insect Techniques - Genetically Modified Mosquitoes, CDC, Accessed 2021.

[20] Gideon A. Ngwa, Miranda I. Teboh-Ewungkem, Yves Dumont, Rachid Ouifki, Jacek Banasiak, On a three-stage structured model for the dynamics of malaria transmission with human treatment, adult vector demographics and one aquatic stage, Theor. Biol. 481 (2019) 202–222, Celebrating the 60th Birthday of Professor Philip Maini.

[21] M.I. Teboh-Ewungkem, Malaria control: the role of local communities as seen through a mathematical model in a changing population-Cameroon, Adv. Dis. Epidemiol. (2009) 103–140.

[22] Center for Disease Control and Prevention, Larvicides, CDC, Accessed 2021.

[23] Peter Dambach, The use of aquatic predators for larval control of mosquito disease vectors: Opportunities and limitations, Biol. Control 150 (2020) 104357.

[24] Thomas W. Scott, Willem Takken, Bart G.J. Knols, Christophe Boete, The ecology of genetically modified mosquitoes, Science 298 (2002) 117.

[25] Miranda I Teboh-Ewungkem, Olivia Prosper, Katharine Gurski, Carrie A Manore, Angela Peace, Zhilan Feng, Intermittent preventive treatment (IPT) and the spread of drug resistant malaria, in: Applications of Dynamical Systems in Biology and Medicine, Springer, 2015, pp. 197–233.

[26] C.A Manore, M.I. Teboh-Ewungkem, O. Prosper, A. Peace, K. Gurski, Z. Feng, Intermittent preventive treatment (IPT): Its role in averting disease-induced mortality in children and in promoting the spread of antimalarial drug resistance, Bull. Math. Biol. 81 (4) (2019) 193–234.

[27] Center for Disease Control and Prevention, Zika Transmission, CDC, Accessed 2021.

[28] Gideon A. Ngwa, Modelling the dynamics of endemic malaria in growing populations, Discrete Contin. Ddyn. Syst. Ser. B 4 (4) (2004) 1173–1202.

[29] Gideon A. Ngwa, Calistus N. Ngonghala, Nchang B. Sama Wilson, A model for endemic malaria with delay and variable populations, J. Cameroon Acad. Sci. 1 (3) (2001) 169–186.

[30] Gideon A. Ngwa, William S. Shu, A mathematical model for endemic malaria with variable human and mosquito populations, Math. Comput. Model. 32 (7) (2000) 747–763.

[31] Ronald Ross, Studies on Malaria, John Murray, London, 1928.

[32] Ronald Ross, The Prevention of Malaria, John Murray, London, 1911.

[33] Jia Li, Discrete-time models with mosquitoes carrying genetically-modified bacteria, Math. Biosci. 240 (1) (2012) 35–44.

[34] Gideon A. Ngwa, Ashrafi M. Niger, Abba B. Gumel, Mathematical assessment of the role of non-linear birth and maturation delay in the population dynamics of the malaria vector, Appl. Math. Comput. 217 (7) (2010) 3286–3313.

[35] Angelina Mageni Lutambi, Melissa A Penny, Thomas Smith, Nakul Chitnis, Mathematical modelling of mosquito dispersal in a heterogeneous environment, Math. Biosci. 241 (2) (2013) 198–216.

[36] S.Y. Tchoumi, Kamgang Jean Claude, D. Tieudjo, Gauthier Sallet, A basic general model of vector-borne diseases, in: Communications in Mathematical Biology and Neuroscience, 2018.

[37] Gideon A. Ngwa, Terence T. Wankah, Mary Y. Fomboh-Nforba, Calsitus N. Ngonghala, Miranda I. Teboh-Ewungkem, On a reproductive stage-structured model for the population dynamics of the malaria vector, Bull. Math. Biol. 76 (2014) 2476–2516.

[38] Romoser William, John D. Edman, L.H. Lorenz, T.W. Scott, Histological parameters useful in the identification of multiple bloodmeals in mosquitoes, Am. J. Trop. Med. Hyg. 41 (6) (1989) 737–742.

[39] P.J. McCall, David W. Kelly, Learning and memory in disease vectors, in: Research Update. Trends Parasito, 18, (10) 2002, pp. 429–433.

[40] Mike W. Service, Harold Townson, The anopheles vector, in: David A. Warrell, Herbert M. Gilles (Eds.), Essential Malariology, CRC Press, Taylor & Francis Group, 2002, pp. 59–84.

[41] Nobuyuki Tsuji, Takao Okazawa, Norio Yamamura, Autogenous and anautogenous mosquitoes: a mathematical analysis of reproductive strategies, J. Med. Entomol. 27 (4) (1990) 446–453.

[42] P.F. Verhulst, Notice sur la loi que la population suit dans son acroissement, Corresp. Math. Phys. 10 (1838) 113–121.

[43] J. Maynard-Smith, Models in Ecology, Cambridge University Press, Cambridge, England, 1974.

[44] W.E. Ricker, Stock and recruitment, J. Fish. Res. Board Cannada 11 (1954) 559–623..

[45] Horst R. Thieme, Mathematics in Population Biology, Princeton, New York, 2003, pp. 421–452.

[46] Christopher JL Murray, Lisa C Rosenfeld, Stephen S Lim, Kathryn G Andrews, Kyle J Foreman, Diana Haring, Nancy Fullman, Mohsen Naghavi, Rafael Lozano, Alan D Lopez, Global malaria mortality between 1980 and 2010: a systematic analysis, Lancet 379 (9814) (2012) 413–431.

[47] Jack K. Hale, Ordinary Differential Equations, John Wiley & Sons, New York, 1969, pp. 296–297.

[48] P. van den Driessche, James Watmough, Reproduction numbers and subthreshold endemic equilibria for compartmental models of disease transmission, Math. Biosci. 180 (2002) 29–48.

[49] Majid Bani-Yaghoub, Raju Gautam, Zhisheng Shuai, P. van den Driessche, Renata Ivanek, Reproduction numbers for infections with free living pathogens growing in the environment, J. Biol. Dyn. 6 (2) (2012) 923–940.

[50] Jim M. Cushing, Odo Diekmann, The many guises of R_0 (a ditactic note), J. Theoret. Biol. 404 (2016) 295–302.

[51] Mark A. Lewis, Zhisheng Shuai, P. van den Driessche, A general theory for target reproduction numbers with applications to ecology and epidemiology, J. Math. Biol. 78 (2019) 2317–2339.

[52] Stephen Wiggins, Introduction to Applied Nonlinear Dynamical Systems and Chaos, second ed., Springer-Verlag, 2003,
[53] Jack Carr, Applications of Centre Manifold Theory, 35, Springer Science, 2012.
[54] L. Michaelis, M.I. Menten, Die kinetik der invertinwirkung, Biochem. Z. 49 (1913) 333–369.
[55] Calistus N. Ngonghala, Jemal Mohammed-Awel, Ruijun Zhao, Olivia Prospe, Interplay between insecticide-treated bed-nets and mosquito demography: implications for malaria control, J. Theoret. Biol. 397 (2016) 179–192.
[56] P.A. Rossignol, J.M. Ribeiro, A. Spielman, Increased biting rate and reduced fertility in sporozoite-infected mosquitoes, Am. J. Trop. Med. Hyg. 35 (2) (1986) 277–279.
[57] Lawrence Perko, Differential Equations and Dynamical Systems, 7, Springer Science, 2013.
[58] David R. Brillinger, The analyticity of the roots of a polynomial as functions of the coefficients, Math. Mag. 39 (3) (1966) 145–147.
[59] Jerrold E. Marsden, Marjorie McCracken, The Hopf Bifurcation and Its Application, 19, Springer Science, 2012.